NATIONAL ACCELERATOR LABORATORY

P.O. BOX 500
BATAVIA, ILLINOIS 60510
TELEPHONE 312 231-6600
DIRECTORS OFFICE

Proposal 0009A

May 28, 1971

Dr. Lynn Stevenson
Lawrence Radiation Laboratory
University of California
Berkeley, California 94720

Dear Lynn:

In response to your presentation to Ned and me just prior to the Washington APS meeting, I discussed with our Program Advisory Committee the status of your plans for an external muon identification and your feeling that you needed some encouragement from NAL to proceed further with the development of a prototype external muon identifier.

I am impressed by the enthusiasm of your group, and I find that there is broad agreement about the desirability for an external muon identifier along the lines that you are interested in developing and testing. I have, therefore, decided to commit NAL support to your effort during FY 72. You may expect such support to be available up to approximately $30,000. By June of 1972, I expect that both you and we will have sufficient evidence at hand to make a firm decision with regard to the further development and construction of a Phase I external muon identifier. If the development goes well, you can expect support from NAL during FY 73 up to an amount like $90,000. It is my understanding that funding at that level would make it possible to mount your Phase I external muon identifier in FY 73. Because of the complicated nature of these plans, I feel that you should negotiate an agreement with Jim Sanford. This will help to define your goals and our joint responsibilities.

As Ned and I have indicated repeatedly to you in the past weeks, we are not yet ready to take definitive action on physics proposals for the use of a 15-foot bubble

Proposal File No. 9A, B, C.
Master
DO
JRS

9C - 155

chamber for neutrino research. We are, in fact, just now planning to call for proposals to use that bubble chamber for neutrino studies.

I hope that these assurances will be sufficient to encourage your group to continue its work towards the development of an EMI.

Sincerely,

R. R. Wilson

cc: Vincent Peterson

NAL PROPOSAL No. 9-A 7/31/70

Correspondent: M. L. Stevenson
Experimental Physics
Lawrence Radiation Lab
Berkeley, Calif. 94720

FTS/Commercial 415-843-6301

Proposal for a High-Energy Neutrino Experiment In The NAL 30 m^3 H_2, D_2 Bubble Chamber

R. Cence, F. Harris, M. Peters, V. Peterson, D. Yount
University of Hawaii

S. Meyer
Northwestern University

M. Alston-Garnjost, R. Birge, G. Goldhaber
J. Kadyk, S. Parker, M. L. Stevenson, G. Trilling
Lawrence Radiation Laboratory

June, 1970

NAL PROPOSAL # 9A

SUPPLEMENT TO NAL PROPOSAL (#9) FOR A HIGH ENERGY NEUTRINO EXPERIMENT IN THE NAL $30m^3$ H_2, D_2 BUBBLE CHAMBER

University of Hawaii (R. Cence, F. Harris, M. Peters, V. Peterson, D. Yount)

Northwestern University (S. Meyer)

University of California, Lawrence Radiation Laboratory (M. Alston Garnjost, R. Birge, G. Goldhaber, J. Kadyk, S. Parker, M.L. Stevenson*, G. Trilling)

July 1970

We wish to respond here to some of the misunderstandings and criticisms of our proposal to make the NAL $30m^3$ bubble chamber a hybrid system consisting of a fifteen radiation length quantameter and a fourteen collision length hadrometer.

I. Why Hydrogen and Deuterium?

We admit that our preference for using these targets is subjective. It is formed from years of observing strange and unexpected phenomena while scanning hydrogen and deuterium bubble chamber film. One is much more likely to struggle for an explanation to a peculiar event if it occurred on hydrogen. When the target nucleus is more complex one can usually invent many superfluous explanations for the event. Therefore, we believe it is essential to study high energy ν and $\bar{\nu}$ interactions on H_2 and D_2 in a bubble chamber where the interaction vertex is seen and the momentum of all charged tracks measured. The understanding of the unexpected H_2 events will aid in untangling peculiar events in D_2. Observations must be made over all possible kinematic variables. Two important questions must then be answered; 1) Which charged track is the lepton, and 2) What is the momentum of the neutral system? The hybrid system provides the answers.

*correspondent

II. Why Build the Hybrid System When Track Sensitive Targets (TST) are Planned for the NAL 30m^3 Chamber?

The motivation that led us to develope the hybrid system was our awareness of how marginal the usefulness of TST's for high energy neutrino plysics became when the size of the NAL chamber was reduced from 100m^3 to 30m^3. The reason for the marginality is that at least two conversion lengths of Ne-H_2 mixture must blanket the TST. When the chamber volume is reduced, the TST volume reduces at a much greater rate. The solid curves of Fig. 1 summarize the effective TST volumes* for 0, 1, 2, and 3π^0 physics as a function of bubble chamber diameter (in feet). The transverse distribution of neutrinos is assumed to be uniform. Pure Ne is used as the blanket. The design using a 12 foot diameter chamber described by Roe et al in NAL proposal number 44 is used as normalization.

Our original proposal (June 1970) for the development of a hybrid system called for an enlargement of the coils to allow the Quantameter to be inserted. We now believe a much better solution both for TST's and for Quantameter accuracy is to enlarge the chamber to fill the space and to slice two feet off the rear portion of the chamber as shown in Fig. 2. The reasons are discussed on pages 8-10 of Appendix 1. The solid curves of Fig. 3 show the fiducial volume of the hybrid system as a function of the bubble chamber diameter for two possible neutrino transverse distributions. The fiducial volume of the hybrid system is defined to be that space in which a neutrino event can occur and all π^0s be detected. The dashed curves of Fig. 3 show the TST effective volumes that could be placed in a truncated sphere of that diameter. The broken curve of Fig. 3 is the estimated bubble chamber cost. This number is based upon \$0.2 million/ft ø incremental coil cost. Chambers within the range of 10' ø to 14' ø will fit in the 22' ø vacuum tank, use the same expansion system, and the same optics.

* "Effective volume" is defined to be the product of TST volume and the probability of converting all γ's of all π^0s.

We add \$0.1 million/ft Ø to take account of added bubble chamber body cost. This brings the total cost differential to \$0.3 million/ft Ø. The percentage bubble chamber-cost-increase per foot Ø is $\approx$ 4.3%/ft Ø. The percentage increase in fiducial volume is 65%/ft Ø for TST's in the truncated spheres and is 30%/ft Ø for the hybrid system. The large percentage increase in TST effective volume per foot Ø is the reason for our belief that the present 12' Ø design is very marginal for TST's.

The hybrid system with a 12' Ø truncated sphere has (12/4.1 = 3) times the effective volume for one π^0 physics with TST's in a complete 12' Ø sphere and (12/2.3 = 5.2) for three π^0 physics. These factors become (12/3.3 = 3.6) and 12/1.6 = 7.5), respectively, for TST's in a truncated 12' Ø sphere.* The cost of the Quantameter is approximately \$0.35 million. In summary, for modest incremental chamber costs (4.3%/ft Ø) great gain in usefulness both for TST's (65%/ft Ø) and the hybrid system (30%/ft Ø) can be obtained. We urge NAL to expand the chamber size to correspond to a truncated sphere of 14 foot diameter (total volume $\approx$ 30m^3).

III. Determination of the Momentum of the Neutral System

The Quantameter

A. How can we determine the γ's energy when we have no information about the showers in the first two radiation lengths? This is a natural question for heavy liquid bubble chamber physicists to ask. The quantameter operates on a much different principle. It is well established that for photons of energy

*The hybrid system has an advantage for doing "no π^0" physics over the bubble chamber without TST's. With "no π^0" events there is an ambiguity where the event can have a π^0 moving directly downstream or directly upstream. The quantameter can rule out the downstream π^0. The upstream π^0 ambiguity usually involves low energy π^0's.

greater than 1 GeV more than 96% of its energy appears in the form of ionization beyond the first two radiation lengths. Details are given in Appendix I.

B. Is the preliminary cost estimate for the electronic readout realistic?

The proposed multi-wire proportional chamber (MWPC, or "Charpak chamber") measures the position (and ionization) of each charged particle in the Quantameter. An area of 25 meters^2 corresponds to $180^\circ \times 90^\circ$ coverage. We assume an average of 10 gaps (5 to 15 gaps, depending on position) of cm each. Thus 250m^2 of area is to be digitized. Position accuracy to ±1 mm in two coordinates is desired; in addition, pulse height to ±3% is required.

Standard techniques (one amplifier/wire) are very expensive. However, recent developments in higher gain in proportional multiplication (Charpak et al, 1970) and delay-line readout (Perez-Mendez et al., 1970)[1] make possible simplifications. The delay-line can readout 500 wires, with one amplifier. Using the positive induced pulses on steps in the negative planes (oriented, say at ±45 deg to the positive wires) one can readout both x- and y-coordinates in a single gap.

A module of 100 cm width and 300 cm height will require about 2000 center wires (at 45°) and two Mylar planes with 2 mm wide aluminized strips to readout x- and y- into orthogonal delay lines. The estimated cost of delay line readout is \$5000/module,[2] including pulse-height; 70 molules would cost about \$350K.

IV. Identification of the Lepton

The primary purpose of the hadrometer is to absorb all hadrons, permitting the muons to pass through and be identified. Further details are given by Mukhin and Yount.[3]

How can the hybrid system deal with mesons that decay into muons? Fast pions of momentum P can decay into muons whose momenta range from 1/2P to P. Thus accurate momentum measurements (±3%) within the H_2-D_2 bubble-chamber should be able to detect more than 90% of π-μ decays within the chamber. Decays outside

the chamber (in Q, or in H, or between) are more difficult to detect, except that for low momenta (<2 GeV/c) π-μ decays will usually give anomalously short ranges in the hadrometer for the measured momentum.

Thus despite the long average pion decay distance from production vertex to the hadrometer center ($\sim$ 5 meters), corresponding to 9% (at 1 GeV/c) to 1% (9 GeV/c) decay fractions, range and momentum measurements will detect most of these π-μ decays. Full use of the H_2 volume for momentum measurements along a suspected muon track is essential.

The "ambiguous" region includes mainly the quantameter (35 cm) and space between quantameter and hadrometer ($\sim$100 cm).

V. Trigger Rate for Quantameter and Hadrometer

The electronics trigger will require (a) an anti against incident charged particles (or charged particles from the upstream coil), (b) one or more tracks passing through the Quantameter and (c) a muon (penetrating particle) leaving the Hadrometer. This signature rejects muons from the shield, cosmic ray muons, neutrino interactions in the Quantameter or Hadrometer, and neutron interactions. It strongly favors neutrino interactions in the hydrogen.

The Quantameters's proportional chamber is continuously sensitive with fast readout which can be combined with scintillation logic to decide on spark-chamber triggers in <1 μsec. Thus the Hadrometer is fired only when the signature is complete.

If the trigger rate exceeds one per burst, it is possible to refine the Quantameter and/or scintillator logic to define the penetrating muon trajectory more precisely. Multiple electronic "events" per burst can be handled if necessary. This would require more than one vidicon camera (with electronic shutter) for the Hadrometer.

VI. Why Don't the Quantameter and Hadrometer Subtend More Solid Angle?

We have the possibility at a later date to increase the hadrometer to cover 180° thereby detecting muons below 4GeV. The addition of a TST cylinder that runs the full length of the chamber can also be added later.

VII. How Does One Take Account of Hadron Interactions in the Quantameter?

Most of the γ's from a π^{o} are confined in a cone of full angle $2/\gamma$. If a charged pion has a large probability of being emitted into this cone then it will pose some problems for us. However, we wish to give some crude arguments to suggest that this is not the case. Under these circumstances we can track the charged hadron through the quantameter, not being bothered by the γ showers, and get a good measure of the energy it deposits in the quantameter.

The argument is based on a fireball type model [4] where one assumes that a substantial number of pions come into thermal equilibrium at a temperature $kT \approx 0.18$ GeV. Their energy distribution is a Planck-like one. The "overlap" problem is best considered in the rest frame of this fireball. Suppose for the moment that all the pions were neutral, each with its γ ray cone subtending a solid angle of π/γ^2. Here γ is the energy of the pion, E, divided by the pion rest energy μc^2. The fraction of the total solid angle, 4π, that is "used up" by all the γray cones is,

$$f = \frac{\langle n_{\pi} \rangle X_o^2}{4} \cdot \frac{\int_{X_o}^{\infty} \frac{1}{X} \frac{\sqrt{X^2 - X_o^2}}{e^X - 1} dx}{\int_{X_o}^{\infty} \frac{\sqrt{X^2 - X_o^2}}{e^X - 1} dx},$$

where, $X_o \equiv \frac{\mu c^2}{kT}$, $X \equiv \frac{E}{kT}$

Evaluation of the integrals yields, $f = \frac{\langle n_{\pi} \rangle}{27}$

Usually, one third of the mesons will be neutral, in which case

$$f_o \simeq \frac{\langle n_n \rangle}{81}$$

Let us consider the worst possible case.

From Fig. 1 of our original proposal (#9) one sees that for $E\nu$ = 50 GeV, $\langle n_\pi \rangle < 15$, $f_o < 0.18$ for 50 GeV nutrinos.

The probability that all charged pions miss these cones is $(1-f_o)^{n_{ch}}$.

for $\langle n_\pi \rangle = 15$ this probability is $(.82)^{(\frac{2}{3}\cdot 15 = 10)} = 0.14$

The probability that all but one pion miss

$$\text{is} = \frac{\langle n_{ch} \rangle !}{(\langle n_{ch} \rangle - 1)!\,1!}(1-f_o)^{\langle n_{ch} \rangle - 1} f_o^1 = \left(\frac{10!}{9!} = 10\right)(.82)^9(.18)$$

$$= (10)(.168)(.18) = 0.30$$

that all but two pions miss is,

$$\frac{\langle n_{ch} \rangle !}{(\langle n_{ch} \rangle - 2)!\,2!}(1-f_o)^{\langle n_{ch} \rangle - 2} f_o^2 = \left(\frac{10!}{8!\,2!} = 45\right)(.82)^8(.18)^2$$

$$= 45(.204)(.0324) = 0.30$$

that all but three pions miss is,

$$\frac{\langle n_{ch} \rangle !}{(\langle n_{ch} \rangle - 3)!\,3!}(1-f_o)^{\langle n_{ch} \rangle - 3} f_o^3 = \frac{10!}{7!\,3!}(.82)^7(.18)^3 = 0.174$$

and so on. Each charged pion that strikes a cone has a probability of e^{-1}=.368 of not interacting in the quantameter.

In the proposal we assumed that the entire final hadron state comes into thermal equilibrium. In this way we obtain an upper limit on the multiplicity. For Pomeranchuk exchange $\langle n_\pi \rangle$ would be much lower than these.

In Table I we summarize for various multiplicities, $\langle n_\pi \rangle$, a) the probability that no charged pion strike within the "γ-cones", and b) the probability that no charged pion interacts in the quantameter within the "γ-cones".

At this stage we feel confident of our ability to deal with this problem.

We intend to demonstrate capability of the Quantameter to perform the function we describe in our proposal by doing a modest experiment.

TABLE I

$\langle n_\pi \rangle$	Probability that all charged pions miss cones	Probability that no charged pion interact within γ cones.
3	0.928	0.928 + 0.0282 + ... = 0.954
6	0.735	0.735 + .087 + .004 + ... = 0.83
15	0.140	0.140 + 0.110 + 0.040 + 0.009 = 0.30

REFERENCES

(1) "Electromagnetic Delay Line Readout for Proportional Wire Chambers", by R. Grove, K. Lee, V. Perez-Mendez, and J. Sperinde, UCRL-19858, July 1970. Appended to this note.

(2) See LRL Engineering Note F.ET-1361 (July 1, 1970), "Digitizing System for Proportional Chambers Using Delay Line Readout", by F.A. Kirsten for component costs ($0.47 per wire for 512 wire chamber), including scalers, amplifiers, and delay line.

(3) A. Mukhin and D. Yount, "External versus Internal Muon Identification in the 15-Foot Bubble Chamber" 1970 NAL Summer Study.

(4) M.L. Stevenson "The Role of the Planck Distribution in Understanding the Constancy of the Transverse Momentum in High Energy Nucleon-Nucleon Collisions NAL Internal Report TM-219, and Y.W. Kang and M.L. Stevenson "Properties of the Neutrino Beams at a 400 GeV Accelerator" TM 217, page 6.

9A-10

24 July 70
RCS

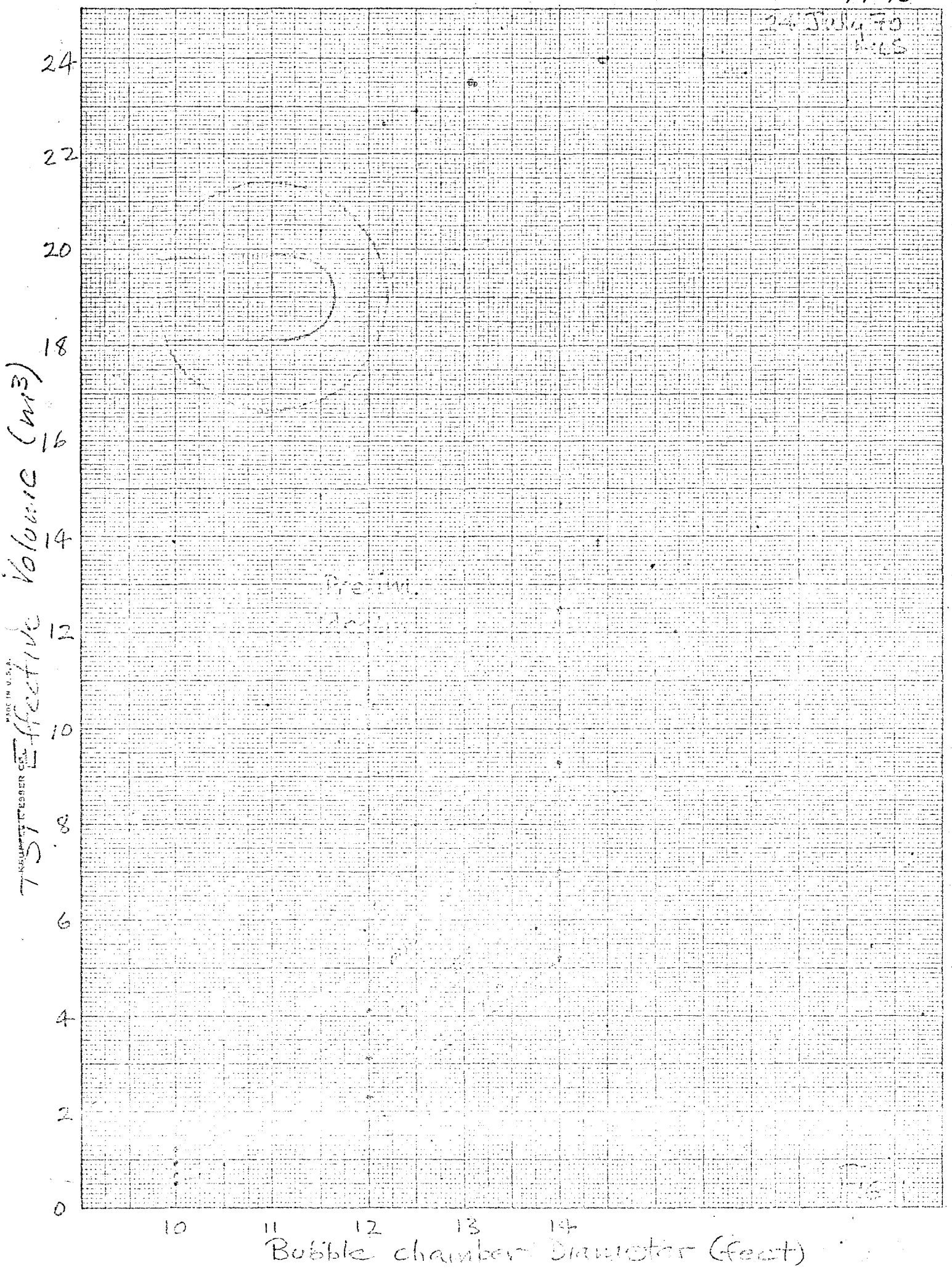

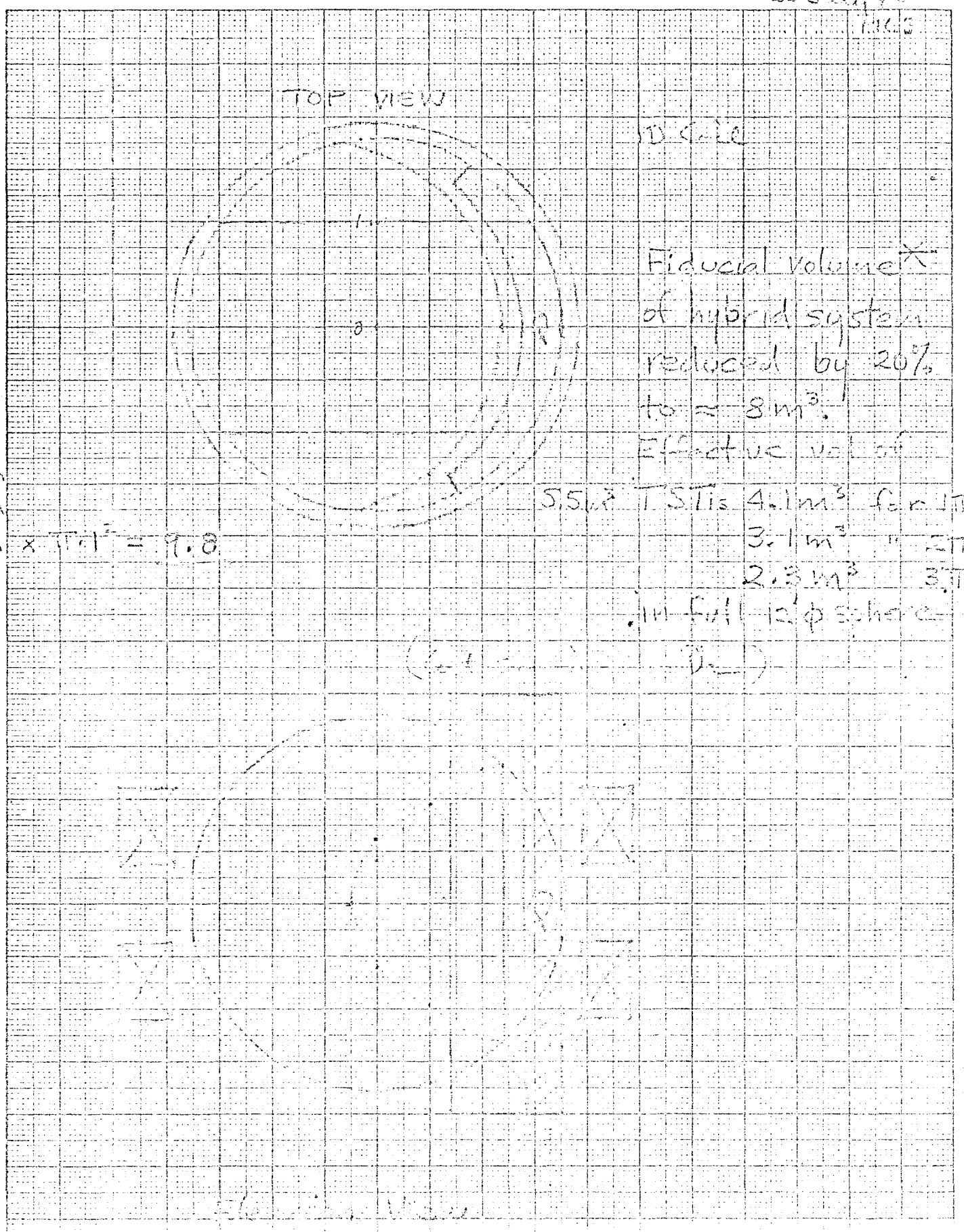

For a shield of approx. the fiducial vol. is a factor of 4 larger.

FIG. 2

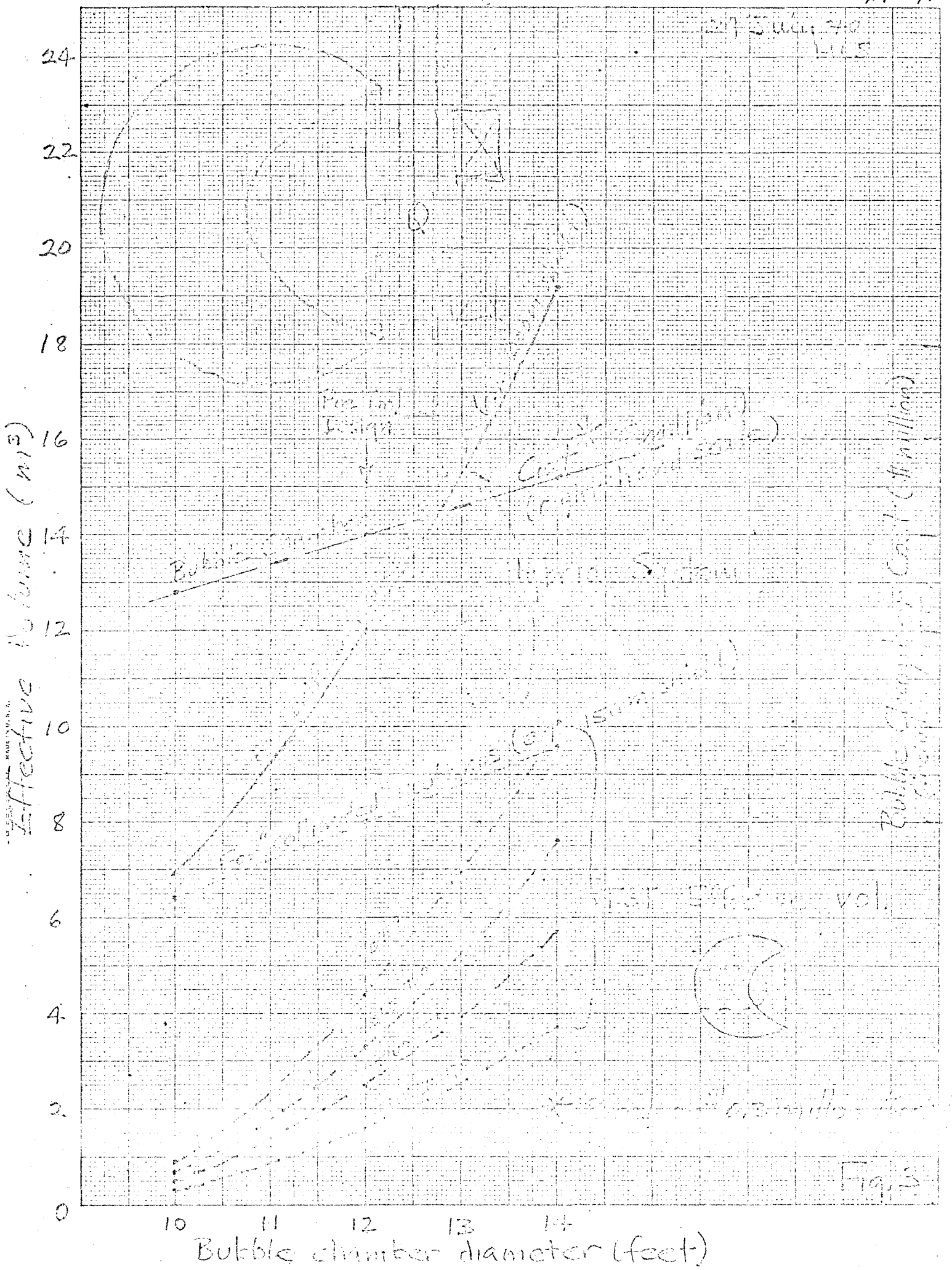
Effective H_2 Volume (m^3)
0
2
4
6
8
10
12
14
16
18
20
22
24
10
11
12
13
14
Bubble chamber diameter (feet)
Fig. 5

APPENDIX 1

M. L. Marcuson

9A-13

PROPORTIONAL QUANTAMETER FOR THE 15-FOOT BUBBLE CHAMBER

D. Yount

University of Hawaii

ABSTRACT

The performance of a quantameter to detect and measure the energy of the neutral pions produced by neutrino interactions in the 15-foot bubble chamber is evaluated.

INTRODUCTION

Since the neutrino energy spectrum is broad, measurement of the νp and νd total cross sections requires that the full energy of each interaction be determined. Essentially, there are four components: charged hadrons, charged leptons, neutrons, and neutral pions. The charged component can be found with high precision (± 3%) from track curvature in the 15-foot H_2, D_2 bubble chamber, although additional equipment is required to identify leptons, particularly muons, with good efficiency. The neutron component may be small for most interactions and can probably be determined with an external hadrometer to sufficient accuracy that the uncertainty in the total energy is not dominated by this source. The most efficient method for measuring the photon energy from neutral pion decay appears to be the lead-plate quantameter: the purpose of this note is to estimate the resolution and precision of this type of detector, thereby emphasizing

the importance of allowing for such a device in the bubble-chamber design.

Typically half the energy in a neutrino interaction appears in the form of charged leptons. Perhaps 1/3 of the total hadron energy appears in the form of neutral pions, which therefore account for 1/6 of the total neutrino energy. The fraction is large enough so that neutral pions must be detected with good conversion efficiency in any total-cross-section experiment; it is small enough so that even a modest accuracy (± 10% of the neutral-pion component) would imply that the dominant error results from track curvature. It may therefore be possible to determine the total neutrino energy to ± 3% in the hybrid H_2, D_2 bubble chamber, while an estimate of ± 5% has been given in an NAL proposal.[1] Corresponding estimates for the neon bubble chamber range as high as ± 20%.[2]

Parallel-plate ionization calorimeters, such as the quantameters[3] widely used in monitoring photon beams, have several intrinsic properties that are essential in determining the neutral-pion energy accurately. First, the response depends only upon the relative ionization in the gas gaps as compared to the ionization in the plates; tolerances of 1% or less in these parameters can be met and insure a uniform response to the same level. Second, since the ratio of gap to plate is independent of track angle in a parallel-plate chamber, such a device is intrinsically isotropic. Third, the output of an ionization calorimeter is linear in the energy absorbed over a wide range.

Fourth, an ion chamber is operated as a one-parameter device; there is one high-voltage setting and one output signal proportional to the total energy deposited in the chamber as sampled periodically via the ionization in the gas gaps. This last feature greatly simplifies the operation of the calorimeter and results in a highly reproducible instrument.

In the case of electromagnetic showers, virtually all of the energy appears ultimately in the form of ions, which are sampled directly in the ionization calorimeter thereby avoiding such questions as the response of scintillation or Cerenkov counters using phototubes. The SLAC quantameter,[4] for example, has been shown to be linear in energy to ± 0.2% from 1 GeV to 14 GeV, the highest energy at which linearity was tested. The response for incident electrons or positrons[5] was found to be the same to about ± 0.3%, and the reproducibility over long periods of time is also on this level. The SLAC quantameter has been calibrated with a Faraday cup so that it can be used as an absolute monitor to a few tenths of one percent. One simply fills the chamber with a standard gas and sets the high voltage.

The precision, linearity, and reproducibility of <u>ionization</u> quantameters under very favorable circumstances are clearly excellent. The performance of a large <u>proportional</u> quantameter in detecting the electromagnetic energy in a single neutrino-induced event from the bubble chamber can be estimated by considering those factors which cause the response to deteriorate, as compared with ordinary quantameters used in beam

monitoring. The analysis below indicates that a statistical uncertainty of ± 3% (1000 tracks for 10 GeV neutral-pion energy) results from shower sampling every 1/2 radiation length, while sampling every radiation length would give ± 4%. When systematic effects are taken into account, the overall accuracy should be better than ± 6% for 10 GeV neutral-pion energy or about ± 1% of the total neutrino energy in a 60-GeV event. Unlike the neon bubble chamber, which has a radius of about 3 radiation lengths, the quantameter improves with energy, the accuracy varying roughly as $1/\sqrt{E_{\pi^0}}$.

SHOWER STATISTICS

The gain of the SLAC quantameter with 1-atm argon-CO_2 filling is about 4000 ions per GeV incident.[4] The copper plates are 0.963 cm = 0.72 radiation lengths thick with an average gas gap of 0.476 cm. An output of about 40 ions/track would result from a single minimum ionizing particle passing through such a gap indicating that the number of tracks sampled is of order 100/GeV. For a total π^0 energy of 10 GeV, 1000 tracks would be expected yielding a statistical uncertainty of about ± 3%. Monte Carlo calculations for electron-photon showers in lead[6] predict about 600 electrons above 1.5 MeV for a 6-GeV shower sampled at intervals of 1/2 radiation length. This is equivalent to 1000 electrons at 10 GeV, consistent with the first estimate. (The quantameter plates are somewhat thicker than 1/2 radiation

length, but particles of less than 1.5 MeV are detected.)

SHOWER SAMPLING AFTER 2 RADIATION LENGTHS

A recent 15-foot bubble-chamber design specifies a thin exit wall of 1/2 inch steel, equivalent to about 0.7 radiation lengths. The front wall of the reentrant tank would be of comparable thickness. Photons originating at the center of the bubble chamber will pass through about 0.3 radiation lengths of liquid hydrogen, so that the total thickness before entering the quantameter is about 1.7 radiation lengths. This may be considered as the first plate of the quantameter, which would begin with a thin window followed by a sensitive gas gap. Since photon cascades are displaced in the direction of the shower axis by about 1 radiation length with respect to electron cascades,[6] photon-shower sampling beginning after 2 radiation lengths should be excellent.

Quantitatively, only about 0.5% of the total ionization in a photon shower at 6 GeV occurs in the first radiation length, while at 1 GeV the value is the same to 0.2%. Less than 4% of the ionization occurs in the first two radiation lengths, the difference in 1 and 6 GeV being less than 1%. The shower multiplicities versus thickness in lead for these two energies are shown in Figure 1 to illustrate this point.[6] Since the quantameter will be calibrated, only the linearity is in question: this appears to be of order 1% for photons above 1 GeV, even

if sampling begins after 2 radiation lengths. Clearly, it makes negligible difference if 10 GeV reaches the quantameter as two photons or a dozen. In fact, the thickness after which sampling begins can be varied from 0 to 2 radiation lengths without affecting the quantameter output by more than 4%.

SHOWER PENETRATION

The shower penetration in percent depends on the incident photon energy and could affect the energy linearity if the quantameter is too thin. About 7% of the ionization in a 6-GeV photon shower occurs after 15 radiation lengths, while less than 2% appears after 20 radiation lengths.[6] In ionization quantameters,[3] the spacing of the last gas gap is usually made large enough to "compensate" for shower penetration, reducing this loss by perhaps one order of magnitude. Compensation is also possible in the proportional quantameter: for example, the gain of the last gap can be increased so that the signal from this gap is proportional to the penetrating ionization rather than simply the ionization of one gap at the particular thickness in radiation lengths. In any case, it is straight forward to design a quantameter for which shower penetration alters the energy linearity by less than 1%. The back-scattered energy from a 6-GeV photon cascade in lead is about 0.12% of the total.[6]

SHOWER DATA

Before considering other systematic effects peculiar to the hybrid application, it is useful to compare the estimates of intrinsic quantameter performance with existing data. An energy resolution of ± 19% (HWHM) has been obtained at 200 MeV by counting sparks in a lead plate chamber with plates 0.15 radiation length thick.[7] Scaling to 1 radiation length and 10 GeV would give

$$19\%/\left[\frac{10\ \text{GeV}}{50\ \text{MeV}} \times \frac{0.15\ \text{r.l.}}{1.0\ \text{r.l.}}\right]^{\frac{1}{2}} = \pm\ 7.4\%$$

as compared with the statistical limit of ± 4%. The scaling is pessimistic for two reasons: 1. tracks observed in a photon shower at intervals of 0.15 radiation lengths are not independent in a statistical sense, and 2. spark counting is less efficient than a direct ionization measurement.

Backenstoss et al.[8] have measured the resolution of a lead-scintillator shower counter consisting of 20 lead plates each 0.8 radiation lengths thick. Their result at 10 GeV is ± 4.9%, which scales to ± 5.4% at 1 radiation length. This value is more applicable to the quantameter configuration than that obtained by scaling track-counting results, but it is still somewhat pessimistic since it involves phototube resolution, light attenuation in plastic scintillator, etc.

Hofstadter and Hughes have studied the resolution in a Pb-NaI array as a function of the thickness of lead.[9] Their results for incident electrons at 8 GeV are shown in Figure 2. The resolution is observed to vary from ± 1% (HWHM) with no lead to ± 6% with 0.75 inches, about 3 radiation lengths, in front of each successive crystal. Since the NaI crystals are 7 inches = 7 radiation lengths thick, the results are not directly applicable to the thin gas gaps of a proportional quantameter. They do, however, illustrate that even very crude sampling of an electromagnetic shower at high energy can yield excellent resolution.

MAGNETIC FIELD

Electrons and positrons from photon conversion in the 0.7-radiation-length exit wall of the bubble chamber must pass through a magnetic field of 30 kG before reaching the quantameter. Since the H_2,D_2 container is spherical and the reentrant quantameter tank cylindrical, as presently envisioned, the distance traveled in the magnetic field depends upon where conversion occurs. A reasonable approximation is

$$s = 5 \text{ cm} + 200(1 - \cos\theta) \text{ cm}$$

where s is the separation, 5 cm is assumed to be the separation in the median plane, 200 cm is the approximate radius of the bubble chamber, and θ is the angle between the median plane and a line from the center of the bubble chamber to the place on the 1/2-inch-steel wall where photon conversion occurs. A track with radius equal to the separation will just miss the quantameter. The momentum cutoff for detection is then given by

$$p(\mathrm{GeV/c}) = 3\ B(\mathrm{kG})\rho(\mathrm{cm})$$
$$= 100s.$$

Values of s and p are plotted versus the height above the median plane of the bubble chamber in Figure 3a.

Assuming the distribution function for the fraction of the total energy given to an electron or positron is constant, energy losses occur in $2(p/p_o)$ of the conversions where p_o is the incident photon energy. The mean energy carried away when a particle is lost is $(p/p_o)/2$ so that the average for all photon conversions is $(p/p_o)^2$. The average energy loss in percent, computed in this way, is plotted versus the height above the median plane in Figure 3b for several photon energies. This model, while exceedingly crude, suggests that measurements of the total π^o energy can be made with accuracy of a few percent or better over most of the quantameter area when the total energy is above a few GeV. The losses in the median plane

are small even at quite low photon energies, and this property could be extended to the entire quantameter by matching bubble-chamber and quantameter geometries, either making the back of the bubble chamber cylindrical or making the quantameter locally spherical. Nine modules 1 m square in a 3 m x 3 m array would approximate a spherical surface nicely if a reentrant tank of suitable shape were made to contain them.

INCIDENT CHARGED LEPTONS

Muons penetrating the quantameter would contribute to the total ionization about one track per gap. For 20 radiation lengths and 40 gaps, this amounts to about 40 tracks/1000 tracks = 4% of the signal from a 10-GeV neutral-pion shower. A correction of this magnitude is straight forward once the penetrating muon has been identified, for example, by a hadrometer in the hybrid system.

Electrons or positrons entering the quantameter will be detected with exactly the same response as incident photons. If the electrons arise from conversion of π^0 photons in the bubble chamber or steel vacuum tank, the resulting signal should be combined directly with that due to π^0 photons, a case already discussed. Electrons from an electron-neutrino ν_e vertex can be identified by associating a shower in the quantameter with

with a charged track in the bubble chamber: spatial resolution in the quantameter is required. The energy of the identified electron can be determined from track curvature in the bubble chamber and can be subtracted from the total quantameter signal, leaving the neutral pion component intact. Dalitz decays are rare and yield pairs of electrons which can be identified in the quantameter and retained in the neutral pion signal.

NEUTRONS AND INCIDENT CHARGED HADRONS

Corrections of order 4% per hadron can be made to the quantameter signal for charged hadrons that penetrate without interacting. No correction is necessary for neutrons that do not interact. For interacting hadrons the correction may be comparable with the neutral pion signal, and it can only be made by analyzing each event in detail, taking into account the incident hadron energy, the penetrating hadron energy (determined, for example, by a hadrometer), and the spatial information provided by the wire readout of the proportional quantameter.

A thickness of 15 - 20 radiation lengths of lead is equivalent to about 1 collision length for strongly interacting particles. Perhaps a third of the energy in each collision goes into neutral pions,[10] which shower and are detected with good efficiency by the quantameter unless the interaction occurs in the last few radiation lengths. Depending upon the

event configuration, it may be necessary to determine the neutral pion component from the neutrino vertex by track counting rather than by measuring the total quantameter signal. Since the sum of the π^0 and interacting-hadron energies is measured absolutely by the quantameter, only the relative numbers of tracks in various showers is required. An accuracy approaching the statistical limit might still be possible in this case, but the analysis would become more complex. A modular quantameter design would substantially reduce the probability for more than one shower signal to occur in a single readout.

SHOWER POINTING ERROR

Experimental data on the accuracy with which the direction of a photon shower can be determined are shown in Figure 4.[11] The results suggest that the pointing error improves slowly after 1 GeV, while the variation with plate thickness may be $t^{1/2}$. The result, scaled to a plate thickness of 1 radiation length, is a pointing error of about $\pm 10^{\circ}$. This should be sufficient to associate individual showers detected in the quantameter with particular events seen in the bubble chamber when more than one event occurs during an expansion. It would also exclude photons from interactions in the coils upstream of the bubble chamber in most cases and would permit pairs or single electrons and positrons to be associated with photons converting in the

1/2-steel wall of the bubble chamber.

PROPORTIONAL READOUT

The primary ionization from a single electromagnetic shower at 10 GeV is not sufficient to produce a practical signal across the high capacitance of a large parallel-plate quantameter. In the proportional chamber[12] several orders of magnitude additional amplification can be obtained through avalanche formation in the high electric field surrounding wires 20 - 50 u in diameter and spaced 1 - 3 mm apart. In the proportional quantameter[1] shower formation and avalanche multiplication combine to yield a signal across the full capacity of one gap or of one chamber that is comparable with the single-avalanche signal across the capacity of one wire. Furthermore, since a small number of signals are involved in a total-energy measurement, high quality amplifiers can be used to preserve the output linearity and stability. The performance of a proportional quantameter, as compared with an ionization quantameter, appears, therefore, to be limited mainly by such considerations as the wire uniformity, the characteristics of avalance formation, and the time distribution and time interval sampled. Each of these effects should be greatly reduced in the statistical average over 1000 tracks. A rough guess is that collection times of several tens of nanoseconds would be sufficient to permit reproducibility, uniformity, and

energy linearity approaching the statistical limit (± 4% for 1-radiation-length plates at 10 GeV).

DISCUSSION

It appears that a lead-plate proportional quantameter of 15 - 20 radiation lengths thickness and a similar number of gaps could be used to determine the neutral-pion energy from individual neutrino interactions in the 15-foot bubble chamber with an accuracy well under ± 10%. Certain classes of events, particularly those in which hadrons interact in the quantameter, would require detailed analysis, including shower-track counting, before this level could be reached. Since on the average only 1/6 of the energy in a neutrino interaction is expected to go into neutral pions, an uncertainty as large as ± 10% in this component would contribute a smaller error to the measurement of total neutrino energy than results from track curvature in the H_2,D_2 bubble chamber, ± 3%. In this sense, it seems clear that a lead-plate proportional quantameter would be highly useful, even if its resolution is several times worse than presently seems feasible.

REFERENCES

1. M. L. Stevenson et al., "Proposal for a High-Energy Neutrino Experiment in the NAL 30 m^3 H_2,D_2 Bubble Chamber," NAL Proposal Number 9.

2. C. Baltay, R. B. Palmer, and N. P. Samios, "Search for the Intermediate Boson, Lepton Pair Production, and a Study of Deeply Inelastic Reactions Utilizing High Energy Neutrino Interactions in Liquid Neon," NAL Proposal Number 53.

3. R. R. Wilson, Nucl. Instr. 1, 101 (1957).

4. D. Yount, Nucl. Instr. Methods 52, 1 (1967).

5. D. Yount, Symposium on Beam Intensity Measurement (Daresbury, England, 22-26 April 1968, V. W. Hatton (Ed.)) pp. 75-96. (See DNPL/R-1.)

6. H. Nagel, Zeitschrift fur Physik, 186, 319 (1965); U. Völkel, DESY Report 65/6, July 1965.

7. R. Cence (Private Communication) July, 1970.

8. G. Backenstoss, B. D. Hyams, G. Knop, and U. Stierlin, Nucl. Instr. Methods 21, 155 (1963).

9. E. B. Hughes, "Observations on the Total Absorption of Electrons and Pions in Matter at GeV Energies," HEPL 603, June, 1969.

10. V. S. Murzin, Progress in Elementary Particle and Cosmic Ray Physics (North-Holland Publishing Company, Amsterdam, The Netherlands, 1967), Vol. IX, p. 245.

11. V. Peterson (Private Communication) July, 1970.

12. G. Charpak, D. Rahm, and H. Steiner, Nucl. Instr. Methods 80, 13 (1970).

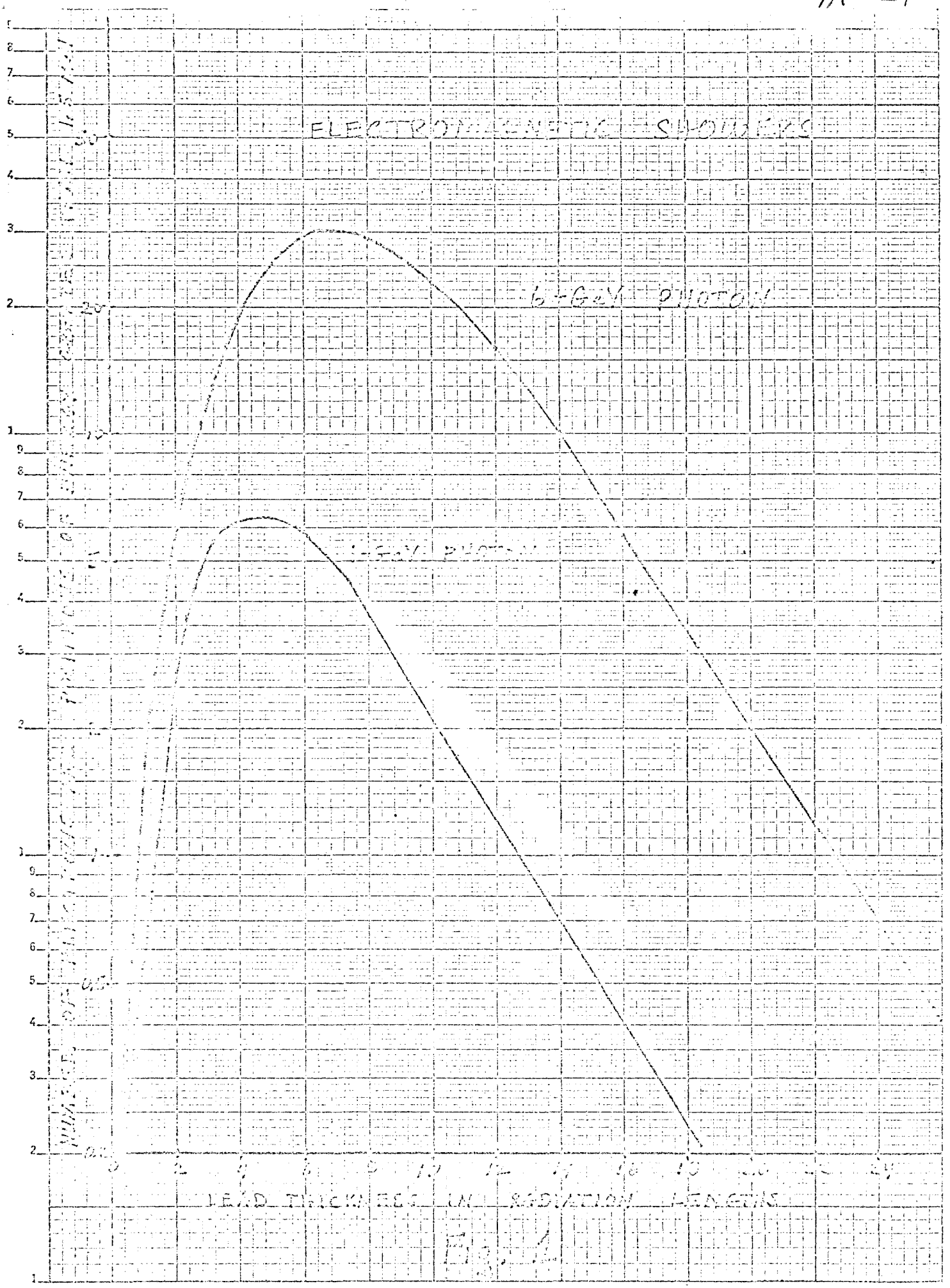
ELECTROMAGNETIC SHOWERS
6-GeV PHOTON
1-GeV PHOTON
LEAD THICKNESS IN RADIATION LENGTHS

Fig. 4

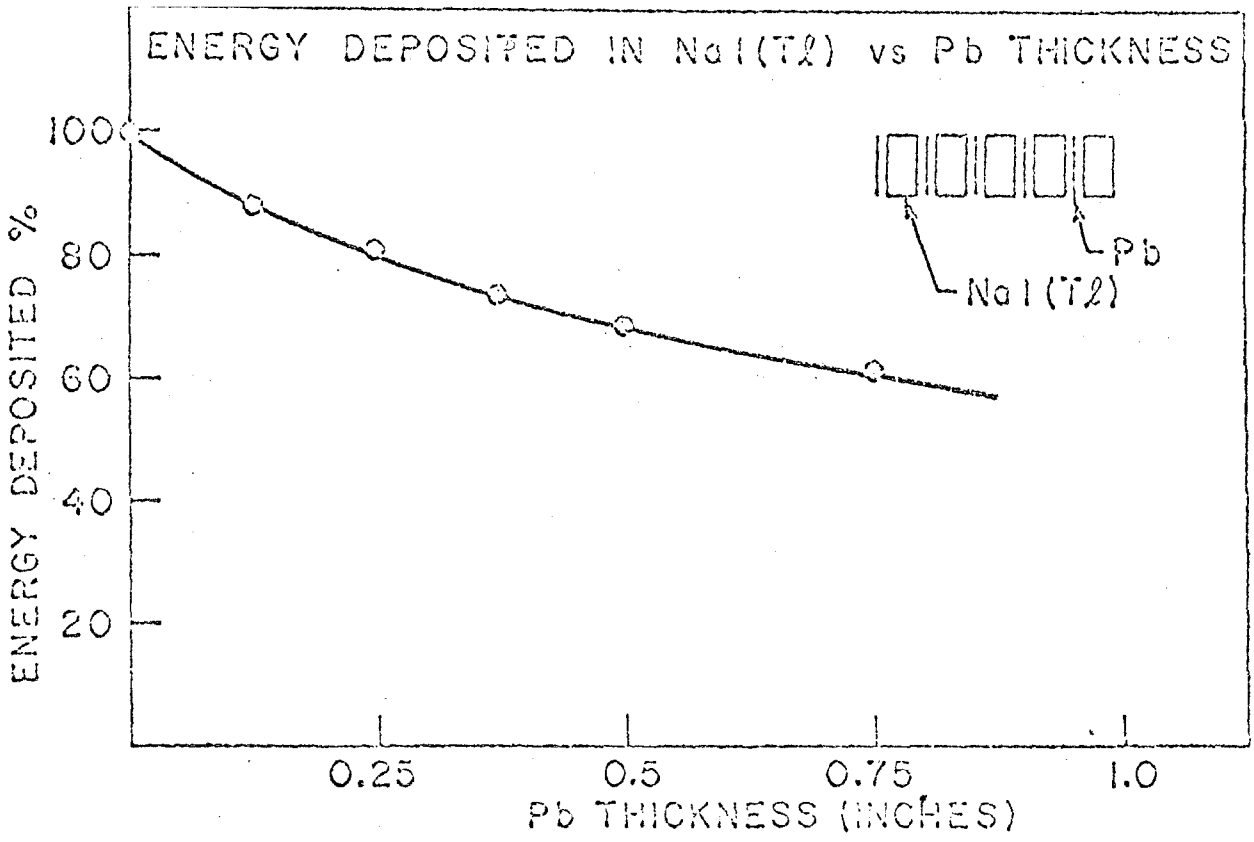
ENERGY DEPOSITED IN NaI(Tℓ) vs Pb THICKNESS
ENERGY DEPOSITED %
100
80
60
40
20
0.25
0.5
0.75
1.0
Pb THICKNESS (INCHES)
Pb
NaI(Tℓ)

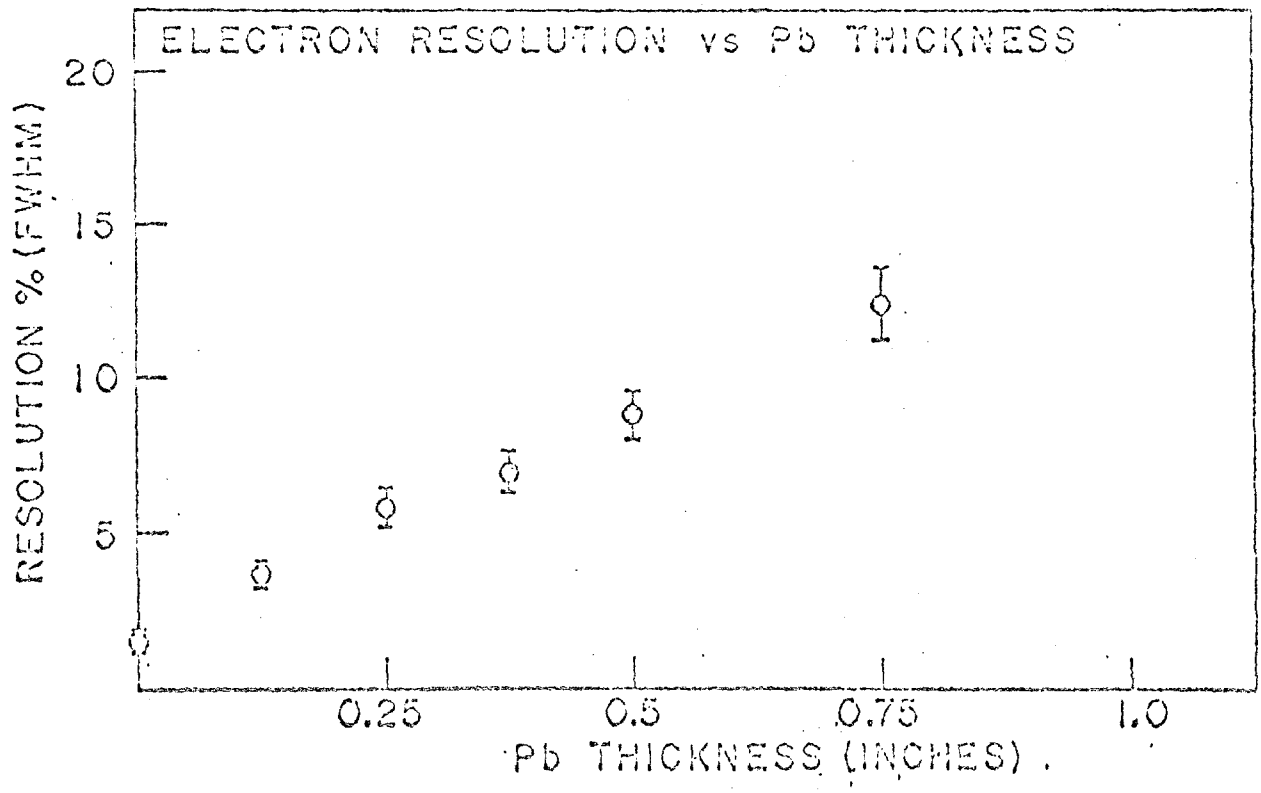
ELECTRON RESOLUTION vs Pb THICKNESS
RESOLUTION % (FWHM)
20
15
10
5
0.25
0.5
0.75
1.0
Pb THICKNESS (INCHES)

Fig. 2

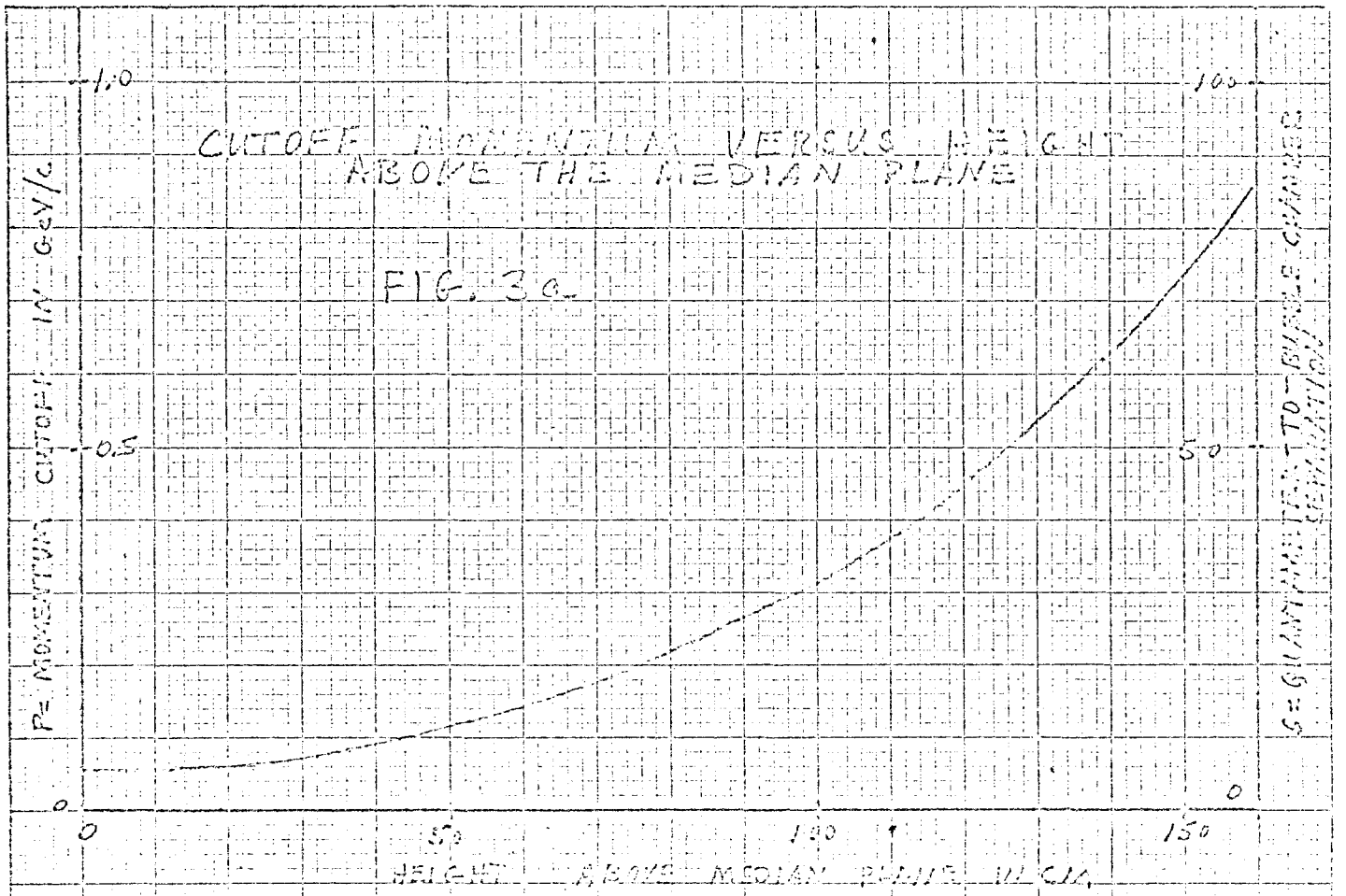
CUTOFF MOMENTUM VERSUS HEIGHT ABOVE THE MEDIAN PLANE
FIG. 3a
P = MOMENTUM CUTOFF IN GeV/c
1.0
0.5
0
100
50
0
0
50
100
150
HEIGHT ABOVE MEDIAN PLANE IN CM.
C = GEOMETRICAL FACTOR - TO - BURST CHANGES

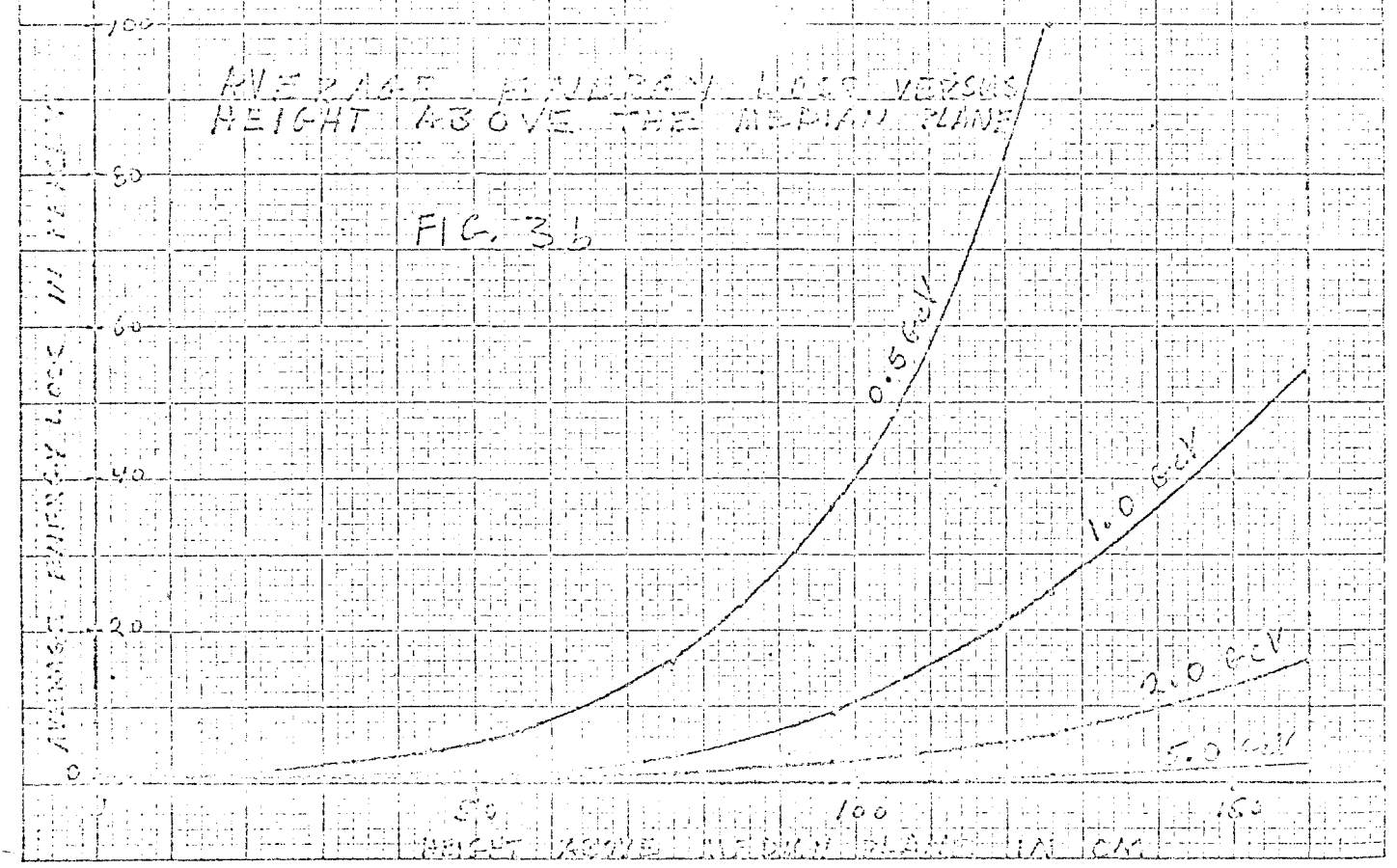
AVERAGE ENERGY LOSS VERSUS HEIGHT ABOVE THE MEDIAN PLANE
FIG. 3b
AVERAGE ENERGY LOSS IN MeV
100
80
60
40
20
0
0.5 GeV
1.0 GeV
2.0 GeV
5.0 GeV
50
100
150
HEIGHT ABOVE MEDIAN PLANE IN CM.

ERROR IN SHOWER DIRECTION IN MRAD
0
50
100
150
PROTON ENERGY IN BEV
0.5
1.0
1.5
2.0
SHOWERS
PHOTONS
RATIO OF MAXIMUM PLATES
0.006 MAXIMUM PLATES
0.016 MAXIMUM PLATES
10-3 MAXIMUM PLATES
FIG 4

Submitted to Nuclear Instruments and Methods

9A-31

UCRL 19858

UNIVERSITY OF CALIFORNIA

Lawrence Radiation Laboratory

Berkeley, California

ELECTROMAGNETIC DELAY LINE READOUT FOR PROPORTIONAL WIRE CHAMBERS

R. Grove, K. Lee, V. Perez-Mendez and J. Sperinde

ELECTROMAGNETIC DELAY LINE READOUT FOR PROPORTIONAL WIRE CHAMBERS*

R. Grove, K. Lee, V. Perez-Mendez and J. Sperinde
Lawrence Radiation Laboratory
University of California
Berkeley, California

June 25, 1970

ABSTRACT

We describe the use of electromagnetic delay lines to read out the position of ionizing events in multi-wire proportional chambers. The delay line used is a ceramic core (non-magnetic) type with a delay of 80 nanosec/cm. The readout accuracy achieved depends on the wire plane which is read out: for the positive plane which forms the electron avalanche, the accuracy is ± 1 mm. (half the wire spacing). For the negative plane, which records the induced signal produced on a number of adjacent wires by the positive ions, the interpolation property of the delay line permits an accuracy of ± 0.15 mm.

I. INTRODUCTION

Multi-wire proportional chambers are now coming into extensive use in nuclear and elementary particle physics. Their main advantage over wire spark chambers is the ability to record events at high rates whereas the spark chambers are limited by the recovery time of the chamber. The main difficulty with wire proportional chambers so far has been the readout--which in the simplest case is done by using an array of amplifiers and storage logic elements connected to the individual wires. In a previous paper[1] we showed that a readout scheme using an electromagnetic delay line could be made which was

considerably cheaper and simpler than the amplifier array method. The delay line that we used was a ferrite loaded delay line to which the individual wires of the chamber were coupled by coils: the positioning accuracy that we were able to achieve was approximately 3 mm. which was the same as the spacing of the wires. In this paper we discuss a similar readout scheme using a different type of electromagnetic delay line without any ferrite or magnetic material in it. This type of delay line has a number of advantages. The ratio of delay to rise time of a pulse and the delay per unit length are higher than in the ferrite line. Furthermore the dispersion of the signal per unit delay is smaller. The combination of these properties makes it possible to use a readout scheme which achieves a position accuracy better than ± 0.15 mm. and can be used in the presence of magnetic fields of any strength.

II. DELAY LINE CHARACTERISTICS

For this project we have been using a commercially available ceramic core delay line of a type that is well described in the literature.[2] Fig. 1 shows the construction of the delay line.[3] The center conductor consists of silver painted longitudinal strips on a ceramic core which is non-magnetic. The outer conductor consists of a copper winding as shown in the figure, made of insulated copper wire 0.09 mm. in diameter with 100 turns/cm. The line is wound in 3 mm. sections with each section overlapping the previous one by 1.5 mm (see Fig. 1 insert). All turns of the winding are in the same direction. This type of delay line has the following characteristics: Delay = 80 nanosec/cm., band pass = 3.6 Mc/sec, attenuation = 1.5 db/microsec delay.

The readout methods described below depend on the high coupling possible through external coils (current coupling) or through external conducting

straps wrapped around the line (capacitative coupling). Both of these coupling schemes are possible due to the fact that the center conductor of the line is operated as the grounded conductor.

The efficiencies of these coupling methods are shown in Fig. 2. Fig. 2a shows the amplitude of the output signal for different rise times of current pulses and various numbers of turns in the coupling coils: Fig. 2b shows the corresponding curves for the capacitative coupling.

An important point to consider is the effect of the external coupling on the delay line characteristics, since we want to maintain an accuracy of timing of the pulses to within 1-1.5 nanoseconds. This loading effect is shown in Fig. 3 for both couplings; it is seen that the capacitative coupling introduces less dispersion and 'ringing' than the coil coupling. Since it is also considerably easier to construct mechanically and electrically, by wrapping plastic with conducting strips etched on it around the delay line, it is the method we prefer to use.

III. PROPORTIONAL CHAMBER MEASUREMENTS

Our measurements were done on chambers with three wire planes: a central plane consisting of wires 25 microns in diameter, spaced by 2 mm. which collected the electrons and whose field gradient produced the avalanches. The positive ion collecting planes were made of wires 100 microns in diameter, spaced by 2 mm. and with the wires oriented at 90° relative to those of the central plane. We collected signals from both the central and the outside planes. The arrangement we used is shown schematically in Fig. 4. For timing purposes we used a zero-cross [4] method.

The positioning accuracy attainable with this delay line depends on the following: (a) the amplitude of the signals above the noise level of the

electronics (b) the polarity and wire spacing of the plane which is being readout. The zero-cross electronics will locate the pulse with a jitter of less than 1 nanosec for pulse amplitudes at the output of the delay line above 400 microvolt. This corresponds to an output of 10-20 millivolts from the chamber wire. This amplitude is attainable with an Argon-Isobutane (70% Ar: 30% Isobutane) gas mixture with the total number of electrons pairs in the avalanche equal to $\approx 5 \times 10^6$.

The accuracy of spatial distribution depends on the polarity of the plane which is being readout due to the asymmetry in the signals induced on the electron collecting wires or on those that receive the displacement current due to the positive ions. Since the signal produced on the delay line is a composite of the signals from a number of wires adjacent to the source of ionization, interpolation between wires is possible if the amplitude of these pulses falls off monotonically with distance. Fig. 5 shows the electric lines of force. An ionizing event will produce an avalanche on wires a or b depending on whether it occurs in the region AA or AB. The position of the avalanche along the wire has a displacement error which is due mainly to diffusion of the electron trajectory due to scattering collisions in the gas. The displacement current signal induced on the positive ion collecting planes centers on the point perpendicularly opposite to the center of the avalanche, since due to the shape of lines of force there is no 'quantizing' effect.

Our measurements confirm this effect, as shown in Fig. 6, in which we plot the position of the ionizing event measured by the delay line, as a function of the position of a collimated source of 5.9 KeV γ-rays from Fe^{55}. The width of the error bars is the full width at half maximum of the distribution observed from the output of the P.H.A. This is due to source width distribution,

jitter in electronic timing and diffusion of the electrons in the gas. The difference in position accuracy and interpolation between the two planes is evident. A proportional chamber with this asymmetry is however quite useful in magnetic spectrometer experiments where the position of the particle trajectories in the plane perpendicular to the magnetic field of the deflecting magnet is usually required to the highest accuracy for the momentum determination.

If symmetry in positional accuracy in two coordinates is desired from one chamber the simplest method is to build it with the positive ion collecting planes oriented at $\pm 45^{\circ}$ relative to the central plane and which are then used for the readout.

The width of the signal pulse on the delay line, relative to the velocity of propagation determines the pulse pair resolution for two simultaneously occurring ionizing events. This is shown in Fig. 7. The results are obtained by simultaneously putting two signals on the delay line and then observing the arrival of the signals at one end of the line. The position of A is fixed and B is moved. The two dashed lines indicate the results which would be obtained for a single pulse at position A or B. Interference between the two pulses will cause the measurements to deviate from the straight lines. In the present setup the two pulse resolution is 30 mm., as can be seen from the figure. We are limited here by the simple zero-cross method of finding the pulse center. Measuring the leading edge of the pulse at each end of the delay line and a suitable coding method would improve the two pulse resolution.

IV. CONCLUSIONS

A delay line readout of the type described above has the advantages

over the individual amplifier per line scheme of greater simplicity and less expense. It is also more accurate due to the ability to interpolate among wires. The two track resolution as noted above is somewhat poorer, but can be improved.

We should also point out that electromagnetic delay lines of this type can be used for reading out wire spark chambers in magnetic fields. The signals from these chambers--current coupled or capacitatively coupled are large enough so that very little amplification is needed.

Acknowledgements

We would like to thank Ray Fuzesy and Herb Steiner for their help and cooperation in constructing and lending us some of the chambers on which these measurements were made.

FOOTNOTE AND REFERENCES

* This work was done under the auspices of the U. S. Atomic Energy Commission.

1) A. Rindi, V. Perez-Mendez and R. T. Wallace, Nucl. Inst. and Methods 77 (1970) 325.

2) J. Blewett, Proc. IRE 35 (1947) 1580; W. J. Carley, Tele-Tech. and Electronic Industries 13 (1954) 74.

3) 'Mini Lines' manufactured by Columbia Technical Corp, 24-30 Brooklyn-Queens Express Way, West Woodside 77, New York.

4) We used type T140/N zero-cross discriminators manufactured by Edgerton, Germeshausen & Grier, Inc., 160 Brookline Ave., Boston, Mass., U.S.A.

FIGURE LEGENDS

Fig. 1. Perspective view of ceramic core delay line.

Fig. 2. Efficiency of coupling from the chamber to the delay line as a function of the input pulse rise time for (a) coils of 50, 75 and 100 turns and (b) copper straps 1 mm. and 2 mm. wide.

Fig. 3: Loading effect of coupling on a 10 cm. delay line for (a) capacitative coupling and (b) coil coupling. The delay lines are loaded with coils or straps, one every two millimeters.

Fig. 4: Block diagram of the electronics used for timing the pulse. The delay line is capacitatively coupled to the chamber and zero-cross discriminators are used to locate the center of the pulse.

Fig. 5: Electric lines of force in the chamber in (a) the view normal to the central wires showing the origin of the quantizing effect and (b) the view parallel to the central wires. To make the lines of force in (b) as parallel as possible flat strips should be used for the negative plane.

Fig. 6: Measurements of the position accuracy for locating ionizing events as read out by the delay line. Figure 6a shows the event location as a function of position when the delay line is connected to the electron collecting wires. Figure 6b shows a similar measurement with the event read out from the positive ion collecting plane.

Fig. 7: Output pulse separation as a function of the input pulse separation. The dashed lines represent the measured position for a single pulse at A or B.

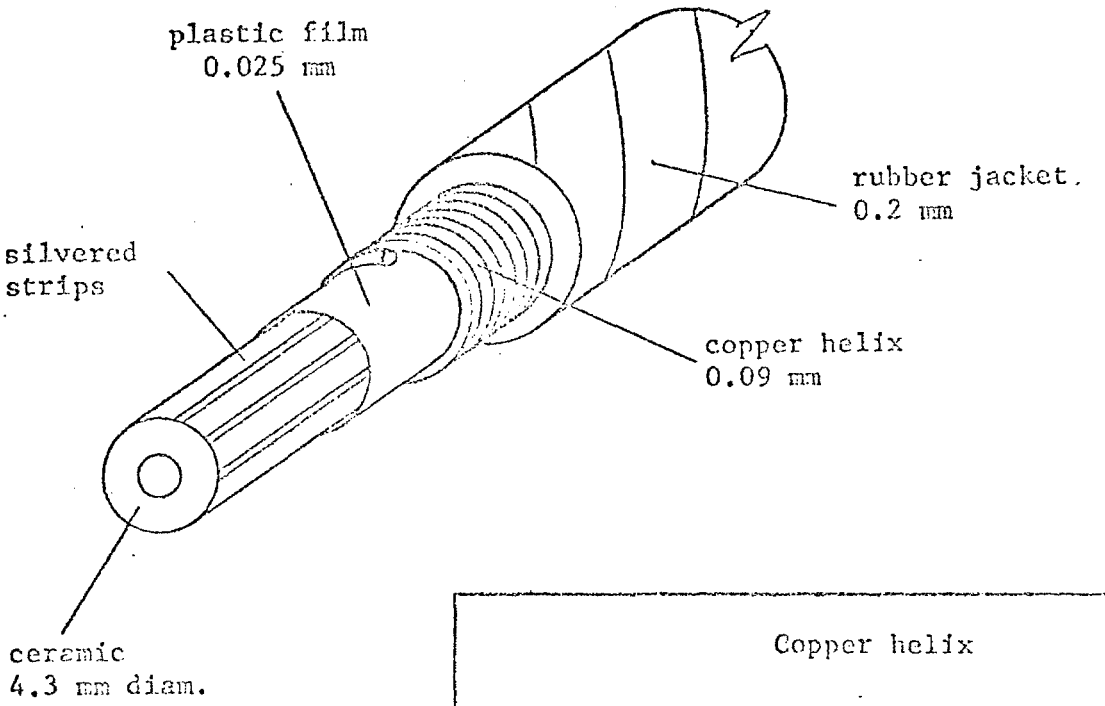
plastic film
0.025 mm
rubber jacket
0.2 mm
silvered
strips
copper helix
0.09 mm
ceramic
4.3 mm diam.

(a)

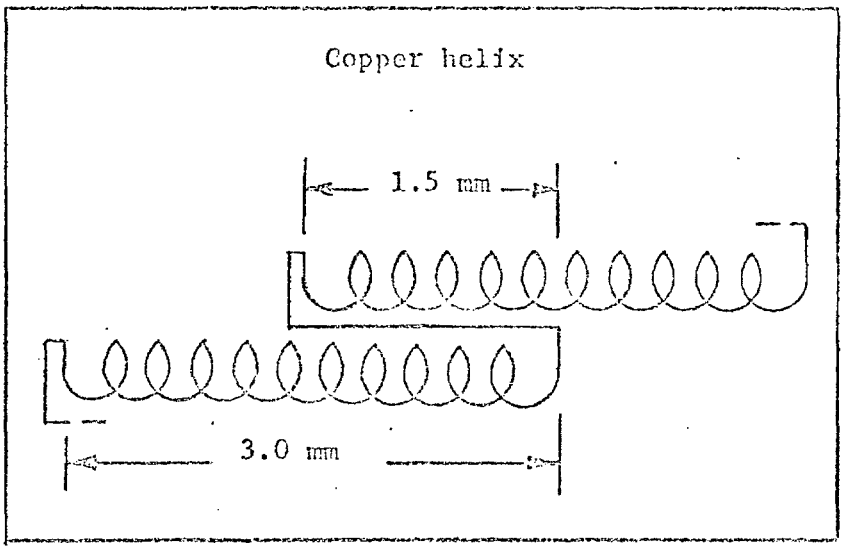
Copper helix
1.5 mm
3.0 mm

(b)

Fig. 1

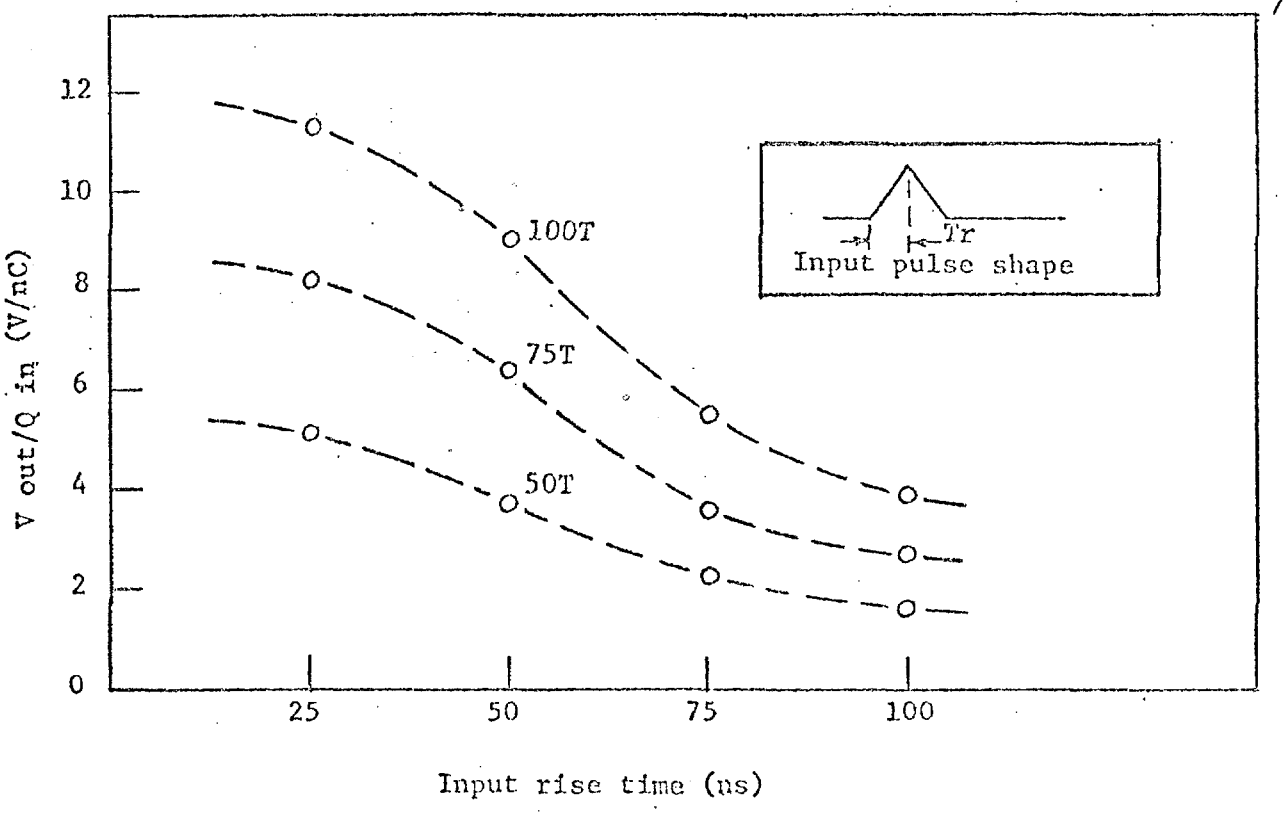
12
10
8
6
4
2
0
V out/Q in (V/nC)
100T
75T
50T
Tr
Input pulse shape
25
50
75
100
Input rise time (ns)

(a)

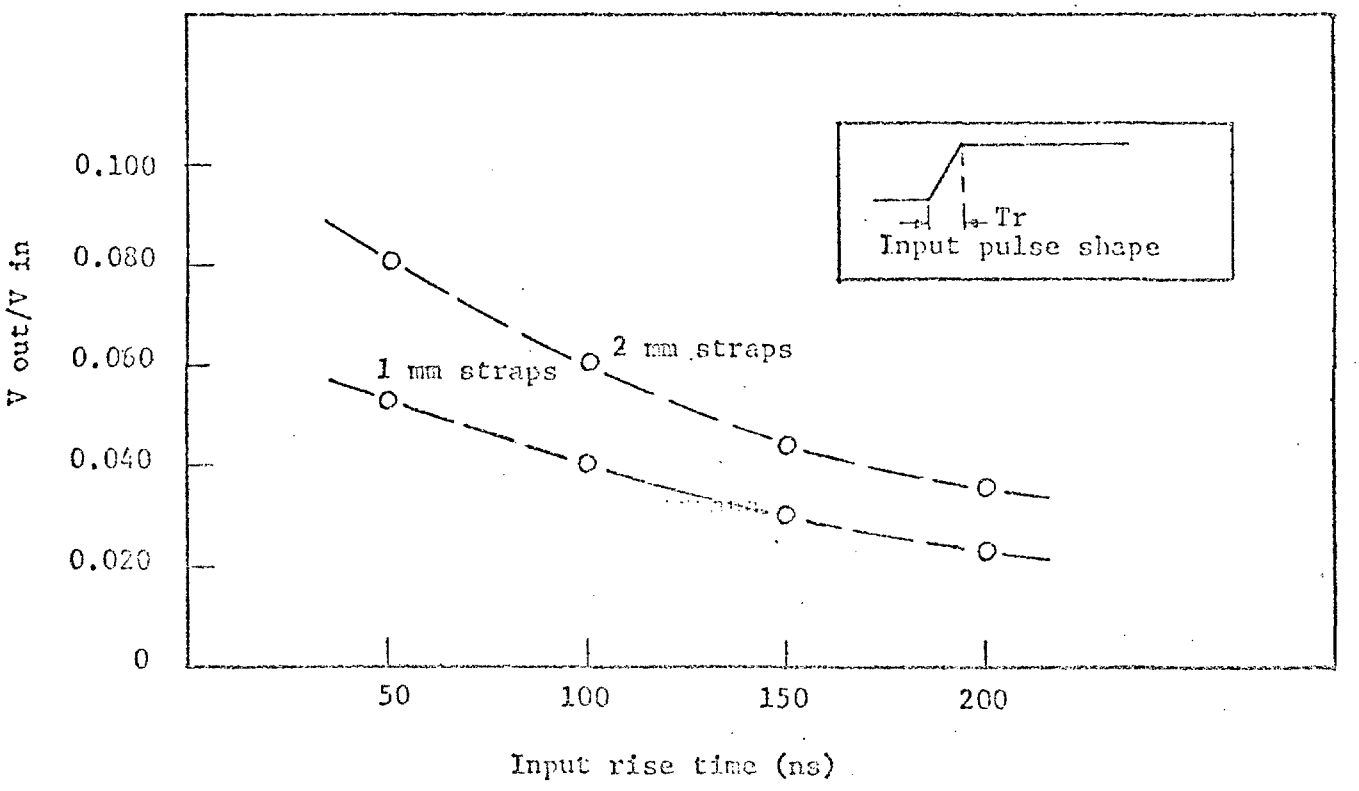
0.100
0.080
0.060
0.040
0.020
0
V out/V in
Tr
Input pulse shape
2 mm straps
1 mm straps
50
100
150
200
Input rise time (ns)

(b)

Fig. 2

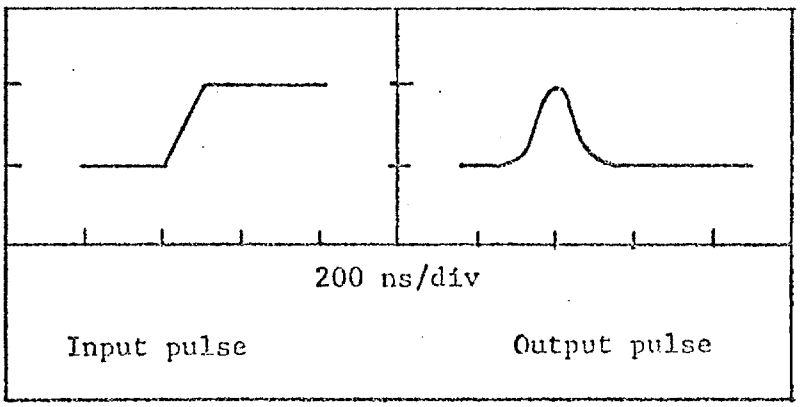
200 ns/div
Input pulse
Output pulse

(a)

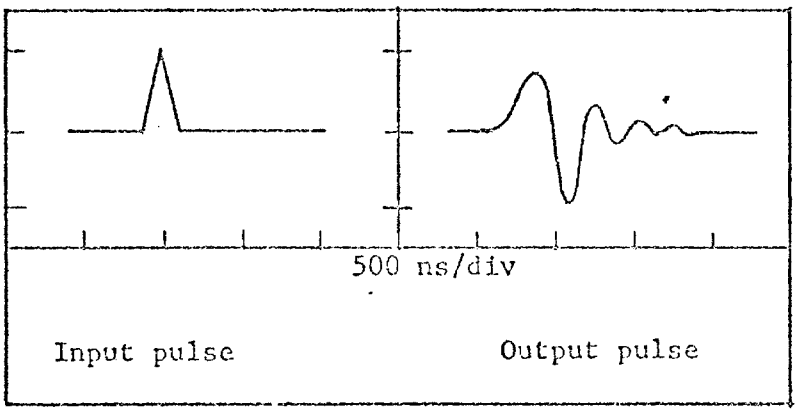
500 ns/div
Input pulse
Output pulse

(b)

Fig. 3

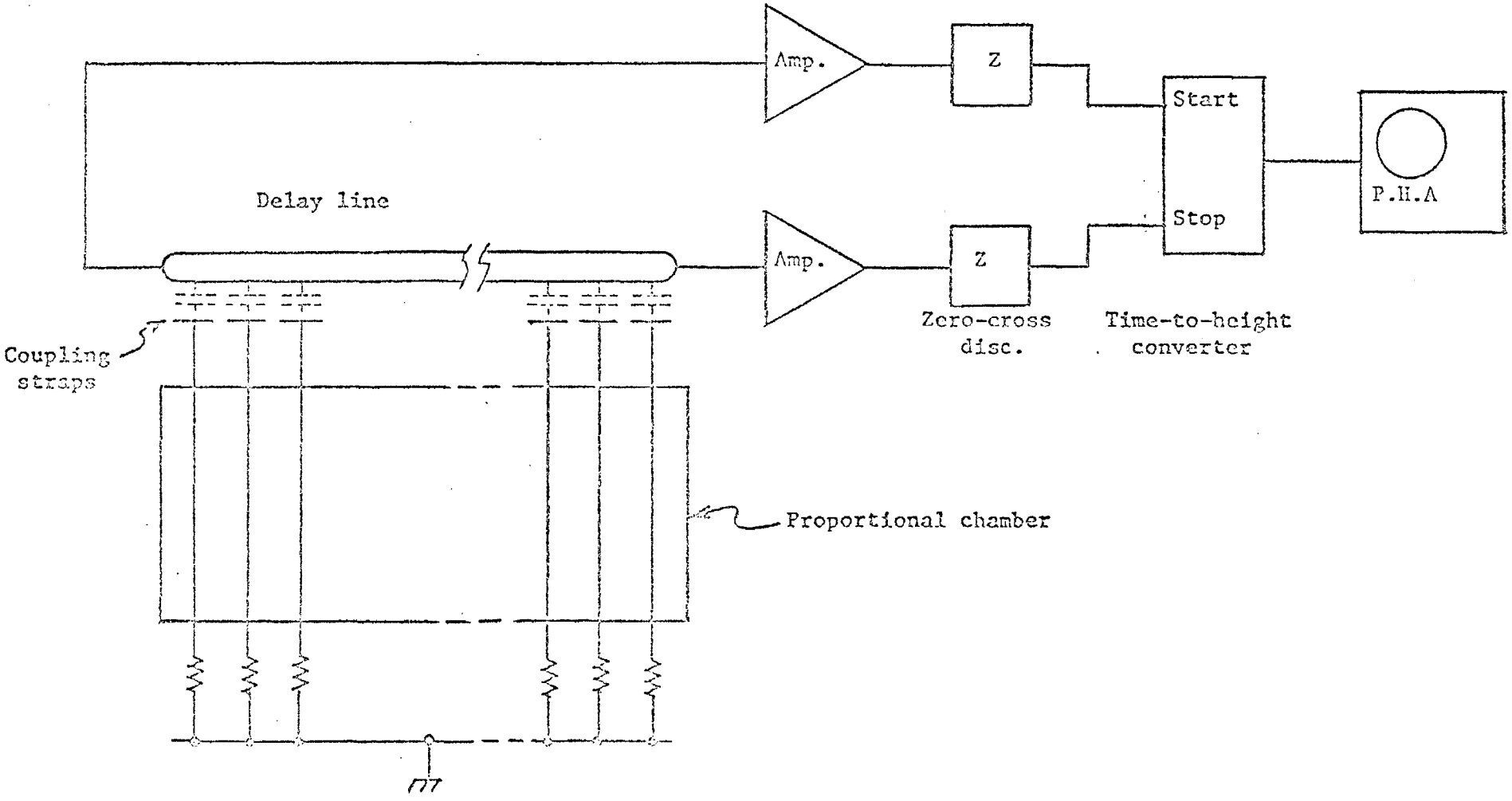
Amp.
Z
Start
Stop
P.H.A
Delay line
Amp.
Z
Zero-cross disc.
Time-to-height converter
Coupling straps
Proportional chamber

Fig. 4

94-43

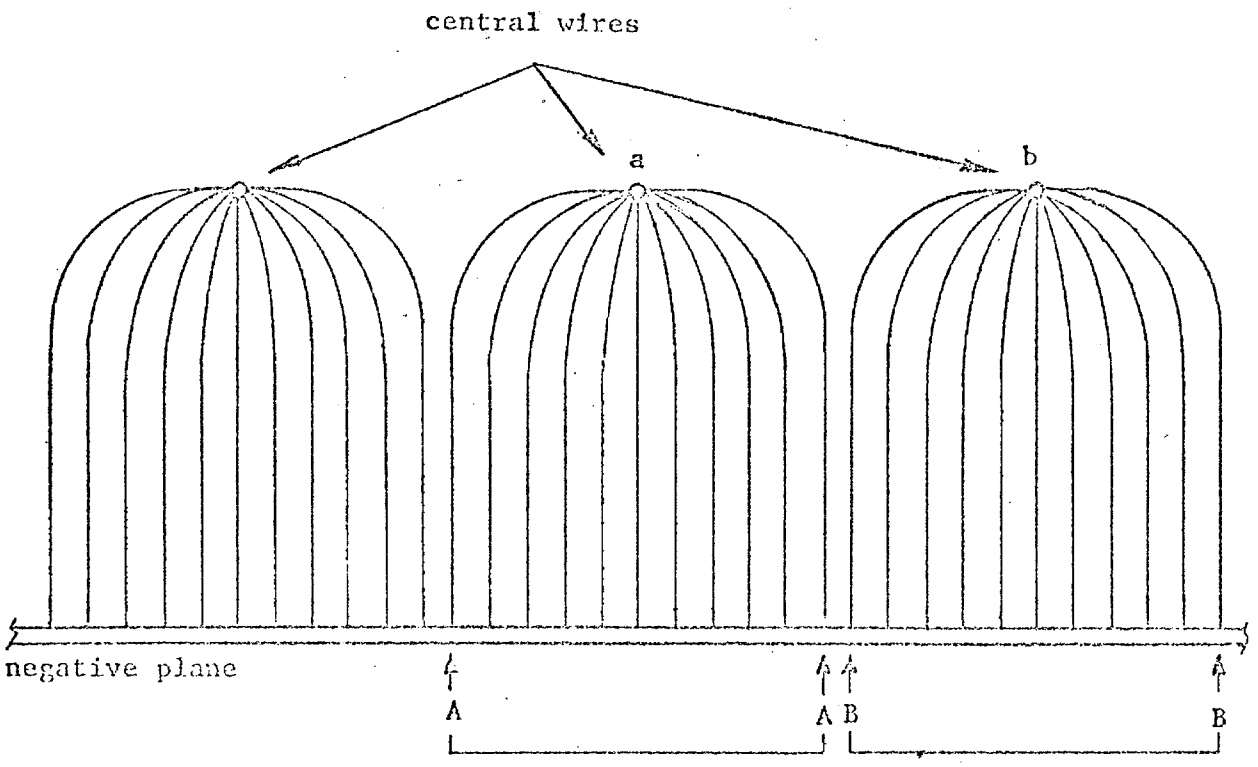
central wires
a
b
negative plane
A
A B
B

(a)

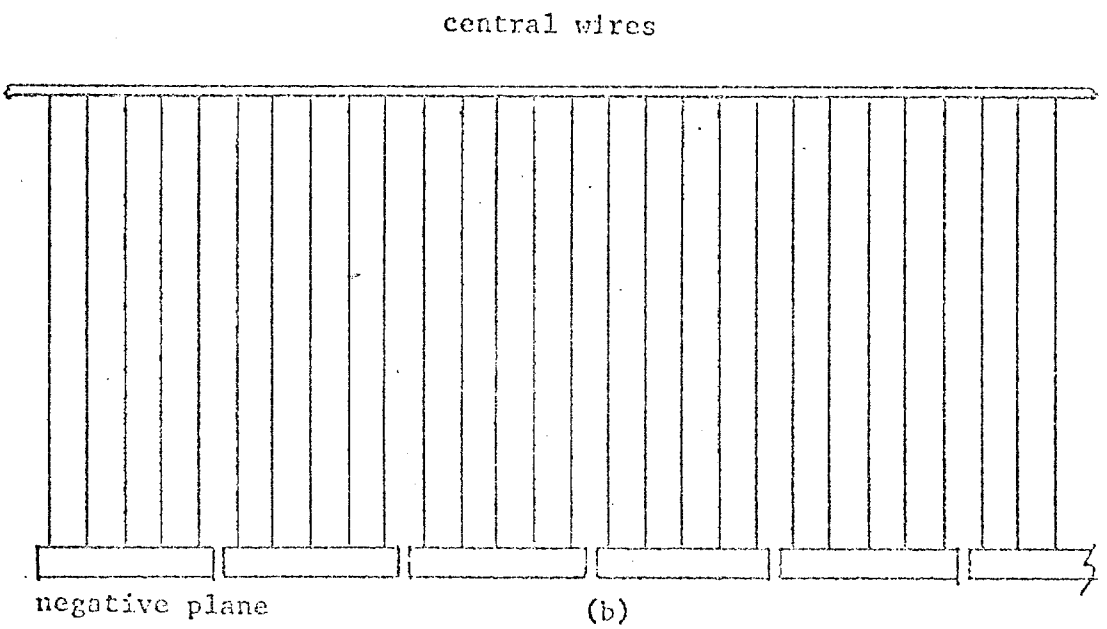
central wires
negative plane

(b)

Fig. 5

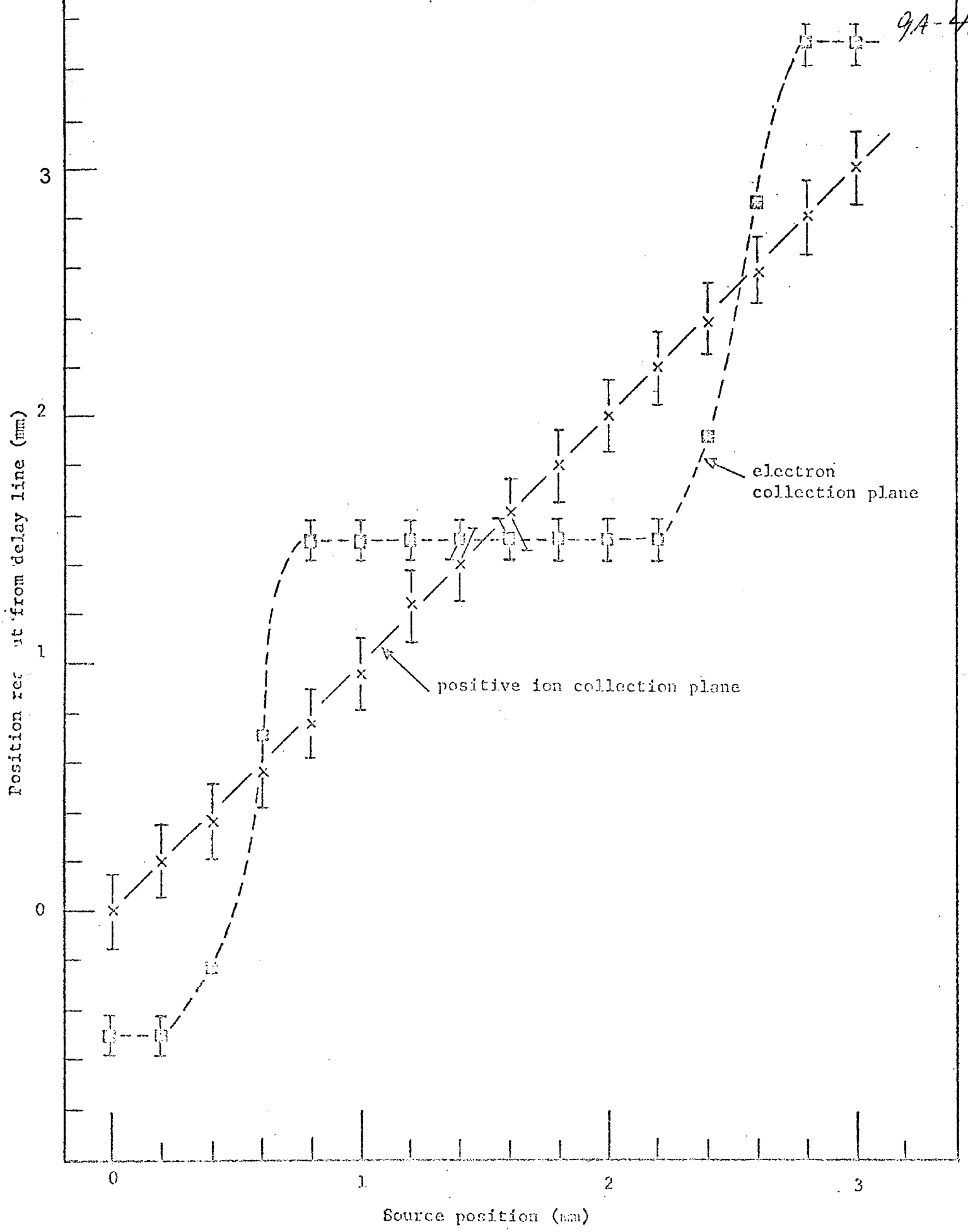
9A-45
3
2
1
0
Position rec ut from delay line (mm)
electron
collection plane
positive ion collection plane
0
1
2
3
Source position (mm)

Fig. 6

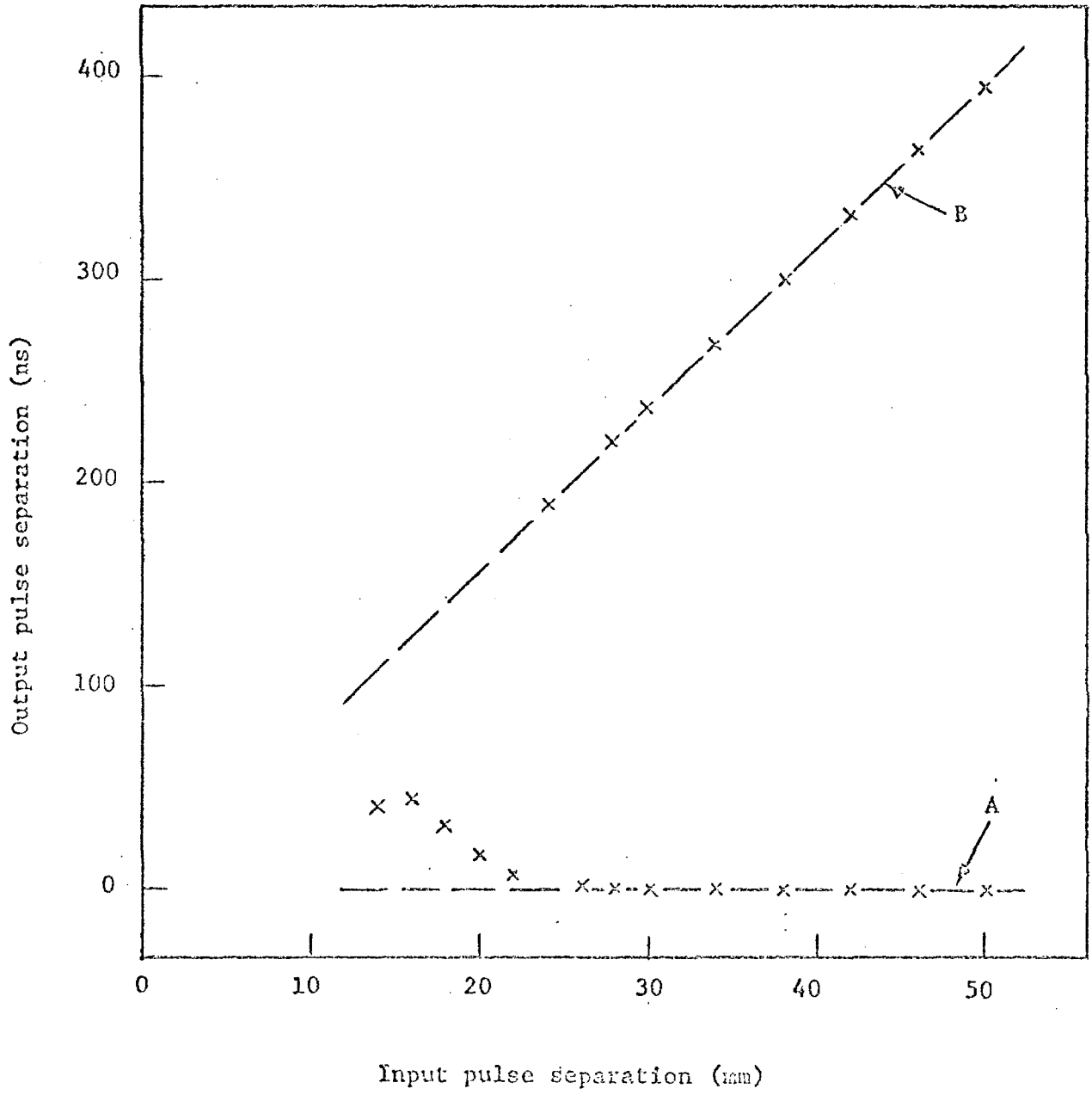
400
300
200
100
0
Output pulse separation (ns)
0
10
20
30
40
50
Input pulse separation (mm)
A
B

Fig. 7

9A-47

NAL PROPOSAL NO. 9B Rev.

Correspondent: M.L. Stevenson

University of California
Lawrence Berkeley Laboratory
Berkeley, California 94720
Telephone: FTS 18-415-843-2740 Ext. 6301

PROPOSAL TO STUDY ANTI NEUTRINO INTERACTIONS IN THE 30 m^3 NAL BUBBLE CHAMBER WITH THE PHASE I EXTERNAL MUON IDENTIFIER

R.J. Cence, F.A. Harris, S.I. Parker, M.W. Peters
V.Z. Peterson, V.J. Stenger
University of Hawaii

A. Barbarro-Galtieri, G.R. Lynch, J.P. Marriner,
F.T. Solmitz, M.L. Stevenson
University of California
Lawrence Berkeley Laboratory

October 3, 1974

9A-48

SUMMARY

We will have analyzed approximately 2500 neutrino interactions by the time the 50,000 pictures test of the Phase I External Muon Identifier (EMI) is completed (E-155). We are now requesting 300,000 pictures of the 15 foot-hybrid*-bubble chamber, filled with hydrogen and exposed to a wide band anti neutrino beam, in order to obtain a comparable number of anti neutrino interactions. We request that at least 50,000 of these anti neutrino pictures be taken during the April-May 1975 run sequence. By that time we will have analyzed 200 neutrino interactions from the copied portion of Experiment 45A film and, hopefully, 500 additional events from the 10,000 picture portion of the above mentioned test sample that we are requesting from the October-November 1974 run sequence. In this way we will make an early comparison of the hadronic final states for neutrinos and anti neutrinos on hydrogen using the wide band beam. This was the original spirit of the deferred portion of our physics proposal 9B (9 July 71) which called for 50,000 wide band events.

Most of the physics arguments and how the kinematics of anti neutrino interactions place constraints on the detectors are contained in that proposal. The first three figures of that proposal are reproduced here. The first summarizes the kinematics, the second shows pictorial momentum vector diagrams to give some idea of what a 20 GeV neutrino interaction might look like. The Landau thermodynamic model[3] was used as a "worst-case" estimate of hadron multiplicity. The third figure summarizes how the muons are bent by the magnetic field and shows why we wanted to place the EMI proportional chambers at 90° azimuth to the neutrino direction.

* With External Muon Identifier. (See reference 2)

Physics Justification

The main purpose of the experiment is to supplement the information that has been obtained by the two counter neutrino experiments,[1] namely to provide detailed information about the hadronic state of anti neutrino interactions. Muon identification is crucial to a clear understanding. The geometrical efficiency of the EMI is greater for anti neutrinos because more of their muons go forward. (See Figs 1 & 3.) Furthermore, any neutrino contamination in the anti neutrino beam can be more readily dealt with if one employs the EMI.

A. Charged lepton current

1. Although, the neutrino energy is low ($\lesssim$50 GeV) we will search for jet-like structure of the "dressed up" recoiling parton and observe how the charge-momentum distribution compares with the corresponding neutrino induced state. It is very important in this analysis to know the direction of the momentum transfer vector. Unless the muon is identified and neutral current events removed from the sample, errors will be introduced into the analysis. (See Fig. 2)

2. The known $(1-y)^2$ dependence of the anti neutrino charged lepton current cross section makes anti neutrinos very useful for searching for the production of rare, massive hadronic states. From Fig. 1, which shows lines of constant hadron invariant mass W, one observes that thresholds for massive hadronic states occur at large y and small x ($\equiv Q^2/2M\nu$) where a paucity of events occurs. Fig. 4 shows, approximately, how the 2500 events will distribute themselves in the x, y space. Here, for simplicity, we have used $\nu W_2 \propto 1-x$. Charmed particles, if they exist, are expected to have leptonic decay modes. Here, again the EMI is useful for detecting its muonic decay mode.

3. Observation of the relative rates of $\Delta S = \Delta Q$ and $\Delta S = 0$ reactions à la Cabibbo, where the final state baryon systems may not be in the same SU(3) multiplet as the proton. For example,

$$\bar{\nu} + p \rightarrow \mu^+ + \left[\Sigma^{0*}(1385) \rightarrow \begin{matrix}\Lambda\,\pi \\ \Sigma\,\pi\end{matrix}\right], \quad \Delta S = \Delta Q$$

$$\bar{\nu} + p \rightarrow \mu^+ + \left[\Delta^0(1235) \rightarrow N\pi\right], \quad \Delta S = 0$$

Here, there is a greater chance for misidentifying the muon than when the baryons are in the same multiplet as the proton. The EMI will eliminate the ambiguity.

4. Test of Adler's relation,

$$\lim_{E_\nu \rightarrow \infty} \frac{d\sigma(\bar{\nu}p)}{dQ^2} - \frac{d\sigma(\nu p)}{dQ^2} = \frac{G^2}{\pi}\left(\cos^2\theta_c + 2\sin^2\theta_c\right)$$

B. <u>Neutral lepton current</u>.

1. Although the neutral lepton current events can be identified in approximately 20 or 30% of the cases we have little chance of being able to determine x and y for them because of our inability to measure the energy-momentum of the neutral portion of the hadronic state. We will, however, try to extract the maximum amount of information from the charged portion. We are submitting a separate proposal to use the EMI with a light mixture of Ne in the hydrogen bubble chamber so as to be able to measure x and y.

2. Neutron background studies are crucial to an ultimate understanding of neutral current physics. We intend to search for anti neutrino interactions in the surrounding super conducting coils where the associated neutron interacts in the bubble chamber. From this we will be able to estimate the neutron background.

C. Possible Surprising Physics

With a detector system that maximizes particle identification, one is best able to detect unusual processes.

9A-52

Apparatus Needed

A. 15' -- Hydrogen filled bubble chamber.

B. External Muon Identifier.

The twenty-five $1m^2$ - multiwire proportional chambers (MWPC) envelope the downstream portion of the 22' diameter vacuum tank. Fig. 5 summarizes the geometrical coverage of the 22 MWPC's used during the July-Aug 74 run of E45A. It shows the vertical and azimuthal coverage as viewed by an observer at the center of the bubble chamber. The plotted points are the predicted hit positions in the MWPC of incoming regenerated muons (from the berm and earth shield) that traverse the visible volume of the bubble chamber. Fig. 6 shows the deviation of the measured position in the EMI from the predicted one.[2] The RMS deviation is very nearly that expected from multiple scattering in the four interaction lengths absorber between the bubble chamber body and the MWPC's. More than 80 percent† of the observed hits fall within the "96% circle" centered at the predicted point. Less than two percent of these incoming tracks interact; consequently, they are mostly muons. Details of this earlier run (400 GeV triplet load) are given in TM513.[2]

C. Neutrino Beam Monitoring Equipment.

D. We would like to assist Experiment 31A (Derrick) in determining the effectiveness of the plug that is likely to be first installed for the April-May 75 run. We plan to operate the EMI during a reasonable fraction of E-31A's exposure in Oct-Nov 74.

E. Scan Projector suitable for monitoring the quality of the bubble chamber pictures from the test strips.

† Some of the beam spill was known to be out of time with the EMI gate during this early run.

Scope of the Experiment

1. 50,000 of 300,000 anti neutrino pictures to be taken during the April-May 1975 run sequence.
2. The remaining 250,000 pictures to be acquired as the schedule permits.
3. At this early stage of bubble chamber operation we shall assume that 30,000 pictures can be accumulated per week. The first 50,000 pictures will take about two weeks, and the remaining 250,000 another eight weeks.
4. Very little testing of equipment is required. We assume implicitly that all beams that are capable of producing neutron or charged background in the bubble chamber will have their spill times not during the bubble chamber sensitive time.

REFERENCES

1. NAL Experiment 21, California Institute of Technology - NAL Group. NAL Experiment 1A, Harvard-Pennsylvania-Wisconsin Group.

2. "Matching 'Muon' Tracks in The 15' Bubble Chamber To The EMI Proportional Chambers", University of Hawaii-LBL Group; Experiment 155, TM-513 (10 October 1974).

"Surveying The External Muon Identifier and The 15' Bubble Chamber With 250 GeV Mesons", TM-509 (16 July 1974), University of Hawaii-LBL Group.

Complete details of the construction and electronics of the MWPC's and an early test of muon identification are found in the following references:

a) NAL Proposal 155, "Development and Test of an External Muon Identifier for the 30 m^3 Bubble Chamber", R.J.Cence, F.A.Harris, S.I.Parker, M.W.Peters, V.Z.Peterson, V.J.Stenger, D.E.Yount; (UH) A.Barbarro-Galtieri, J.P.Marriner, F.T.Solmitz, M.L.Stevenson; (LBL) V.Z.Peterson, Proceedings of 1973 International Conference on Instrumentation for High Energy Physics at Frascati, Italy; "Hybrid Bubble Chamber Detection of Neutrino Events - The External Muon Identifier".

b) "Muon Identification Using Multiwire Proportional Chamber", F.A.Harris, S.I.Parker, V.Z.Peterson, D.E.Yount, M.L.Stevenson; Nuclear Instruments and Methods 103, 345 (1972).

9A-55

c) "EMI Development - Half Meter Proportional Chamber Test Results", S.I.Parker and R.Jones, NAL TM-359, LBL 797, UH-511-122-72.

d) "Digitizing Electronics for the EMI Multiwire Proportional Chambers", E.Binnall, F.Kirsten, K.Lee and C.Nunnally, NAL TM-360, LBL 798.

3) For a recent discussion of this model see J.D.Bjorken and B.L.Ioffe "Annihilation of e^+e^- into Hadrons" SLAC-PUB-1467 (T/E) August 1974. (To be published in Izv. Acad. Nauk, SSSR, Ser. Fiz.)

FIGURE CAPTIONS

Figure 1. The kinematics of inelastic lepton scattering are summarized here. The solid lines radiating from $Q^2=0$, $\nu(=\nu_{max}=E)$ are loci of equal final lepton scattering angle. The parallel solid lines are loci of equal invariant final state hadron mass. They also show "worst case" predictions of hadron multiplicity. The radial line originating at $Q^2=0$, $\nu=0$ are loci of constant $x(=Q^2/2M\nu)$. The dashed curves are loci of constant Lorentz factors, γ_W of the hadron system.

Figure 2. Typical momentum vector diagrams for various regions in the x, y space are shown. The opening angles of the cones are typical of those expected of the Landau Thermodynamical model. A jet-like model would predict opening angles and multiplicities much smaller than these.

Figure 3. Typical Muon Trajectories in the 30 kG field of the 15' chamber are shown. The two solid curves for each (x,y) are the extremes for muons produced in the equatorial plane. The dashed curve is that for a muon emitted with its extreme dip value.

Figure 4. This figure shows approximately how the 2500 anti neutrino events will populate the x,y space.

Figure 5. The azimuthal and vertical coverage of the EMI, as viewed by an observer at the center of the bubble

chamber, is summarized here. It also shows where regenerated muons (from the rear portion of the 1000 meter earth shield) are predicted by the bubble chamber measurements to strike the EMI.

Figure 6. Summary of the deviation of the measured position of muons in the EMI from the predicted position using the bubble chamber picture. x is horizontal and y is vertical.

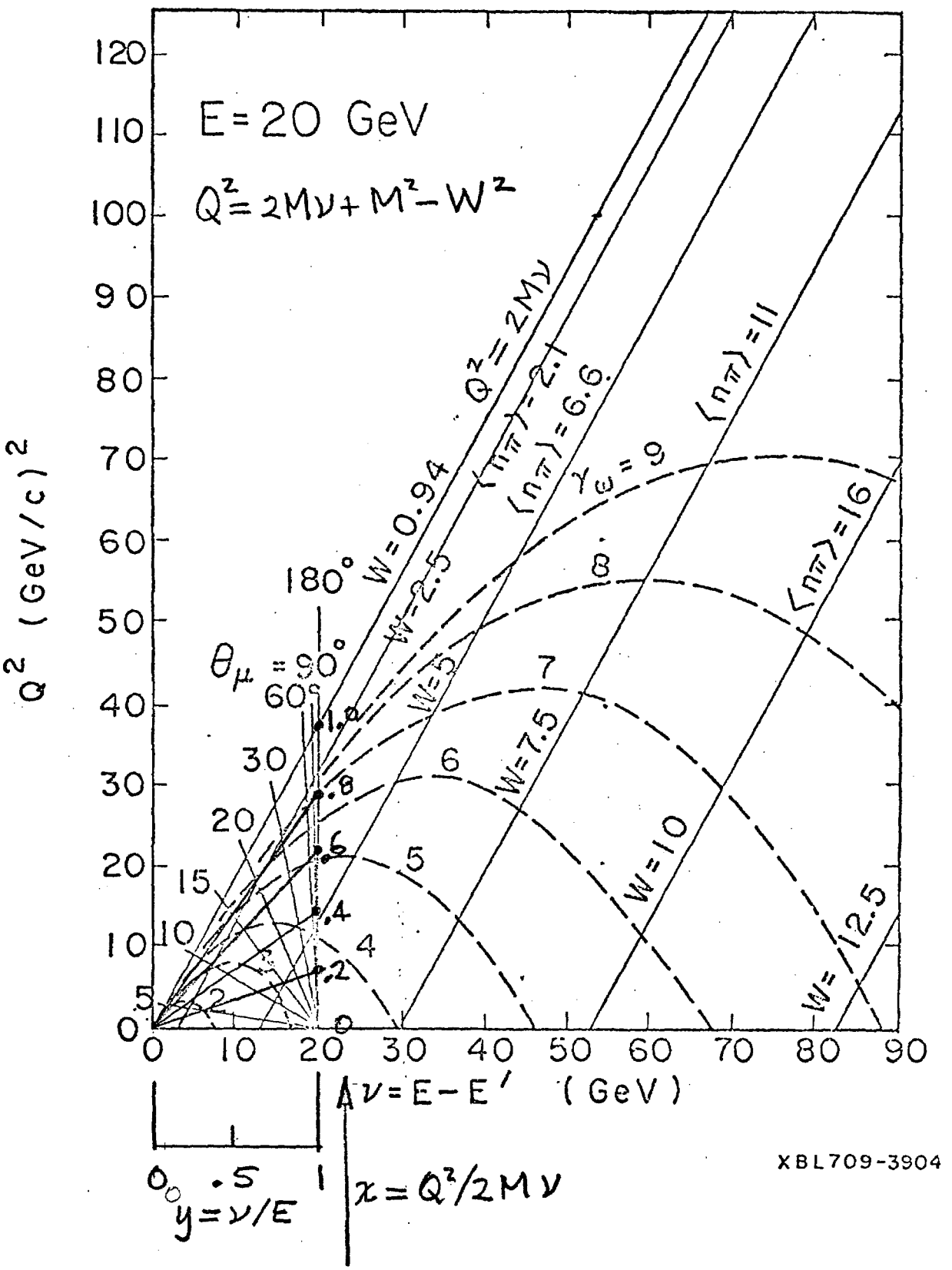
E = 20 GeV
$Q^2 = 2M\nu + M^2 - W^2$
$Q^2 = 2M\nu$
W = 0.94
W = 2.5
W = 5
W = 7.5
W = 10
W = 12.5
$\langle n\pi \rangle = 2.1$
$\langle n\pi \rangle = 6.6$
$\langle n\pi \rangle = 11$
$\langle n\pi \rangle = 16$
$\gamma_\omega = 9$
θ_μ
180°
90°
60°
30
20
15
10
5
2
1.0
.8
.6
.4
.2
0
4
5
6
7
8
Q^2 (GeV/c)^2
$\nu = E - E'$ (GeV)
$x = Q^2/2M\nu$
$y = \nu/E$
XBL709-3904

FIG. 1

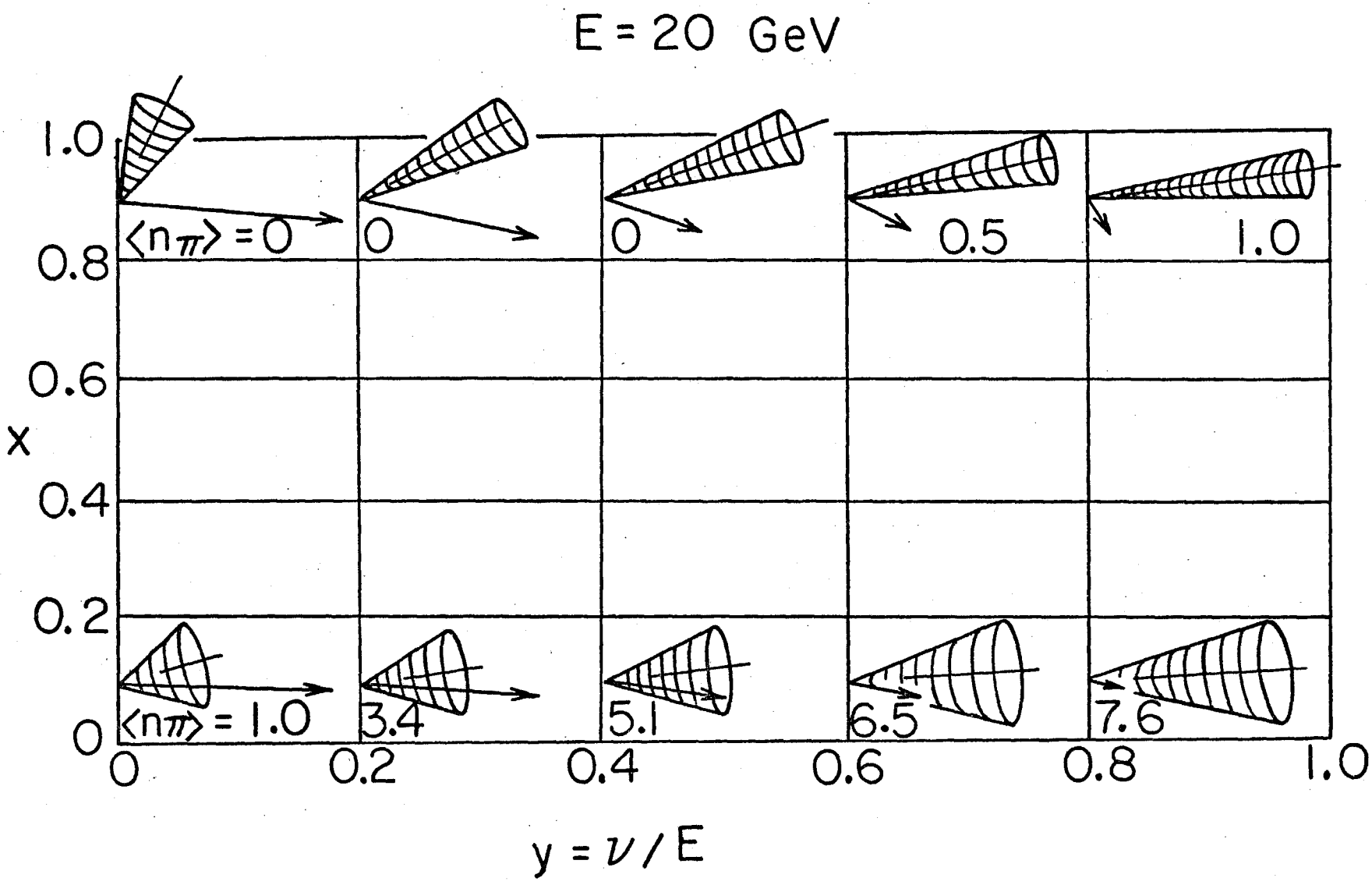

XBL709-3896

FIG. 2

91A-59

Muon Trajectories

$E = 20\,\text{GeV}$

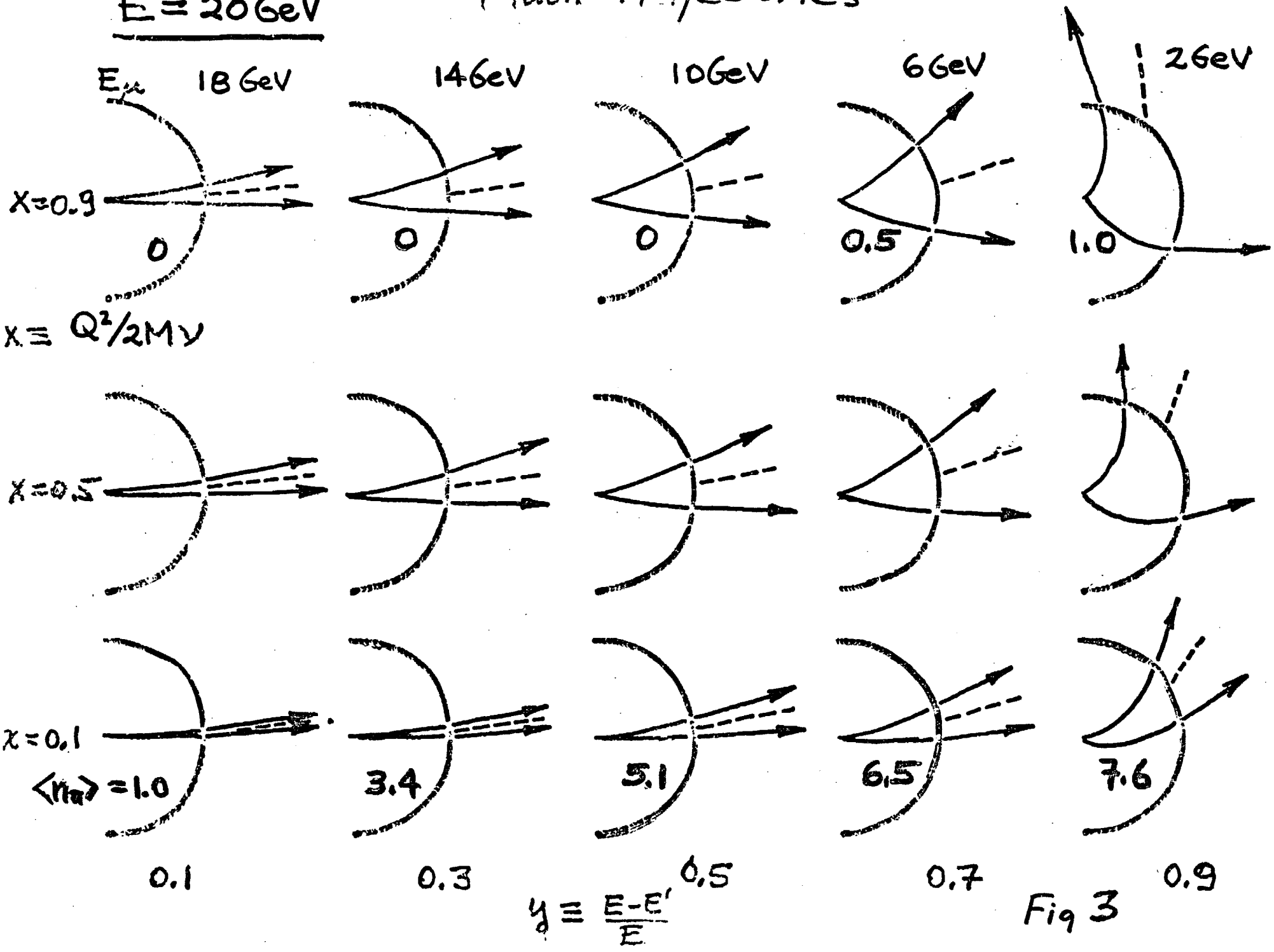

Fig 3

9A-60

Distribution of 2500 events

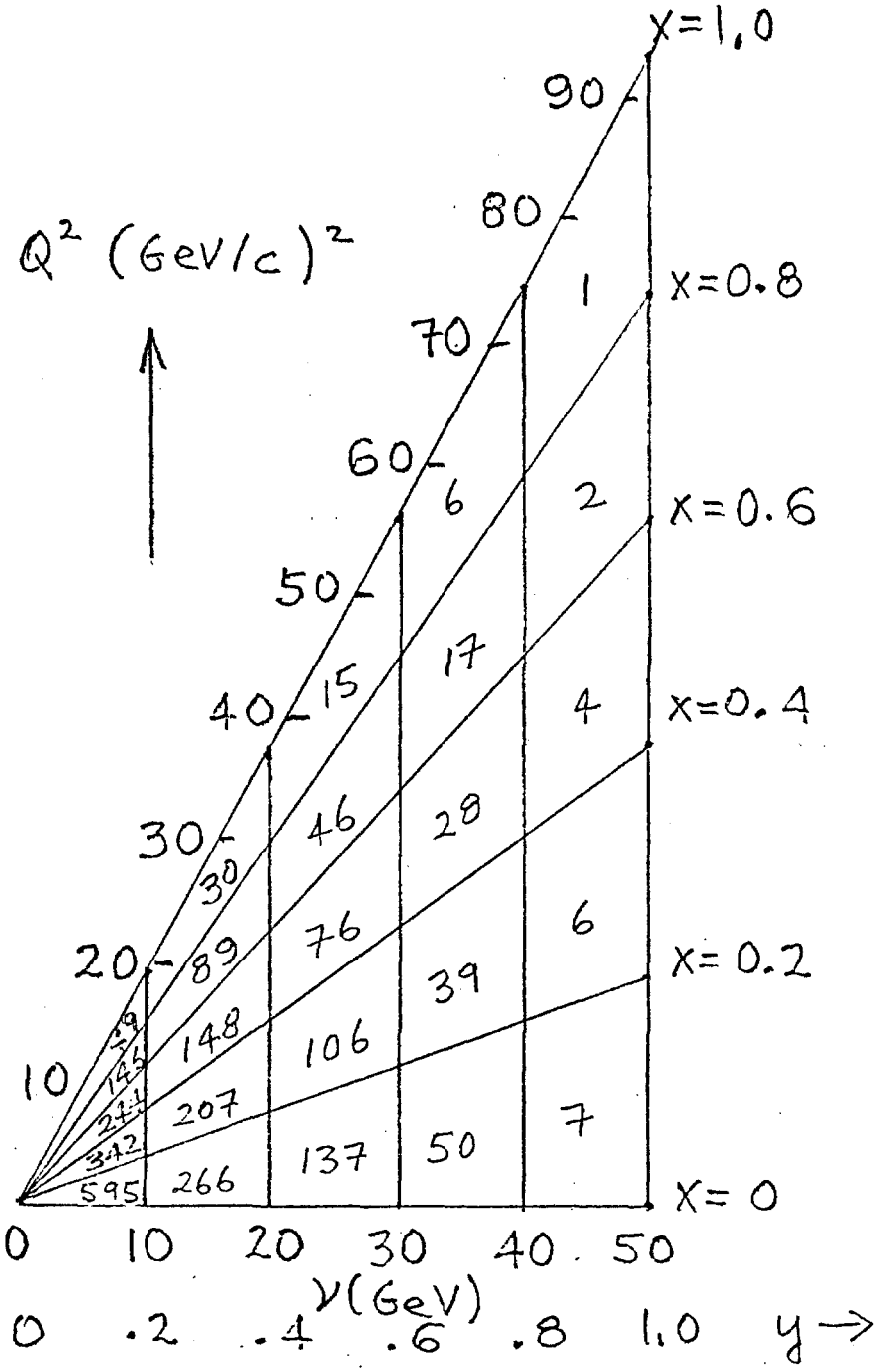

$$\frac{d^2\sigma}{dx\,dy} \approx \frac{G^2 ME}{\pi}\,\frac{Q^2}{2\pi}(1-x)\left\{\sigma_L + (1-y)\sigma_S + (1-y)^2\sigma_R\right\}$$

with $\underline{\sigma_L = \sigma_S = 0}$. $\sigma_{L,S,R}$ ARE HELICITY CROSS SECTIONS

Fig 4

CHAMBER NUMBERS

0	25	20	9	17	21	19	18	0
16	14	4	22	2	15	3	23	0
0	11	8	5	10	7	13	12	0

NUMBER OF HITS

0	0	10	26	46	20	0	0	0
0	4	31	48	68	47	11	0	0
0	2	22	61	49	41	9	1	0

$|p| > 5$ GeV/c

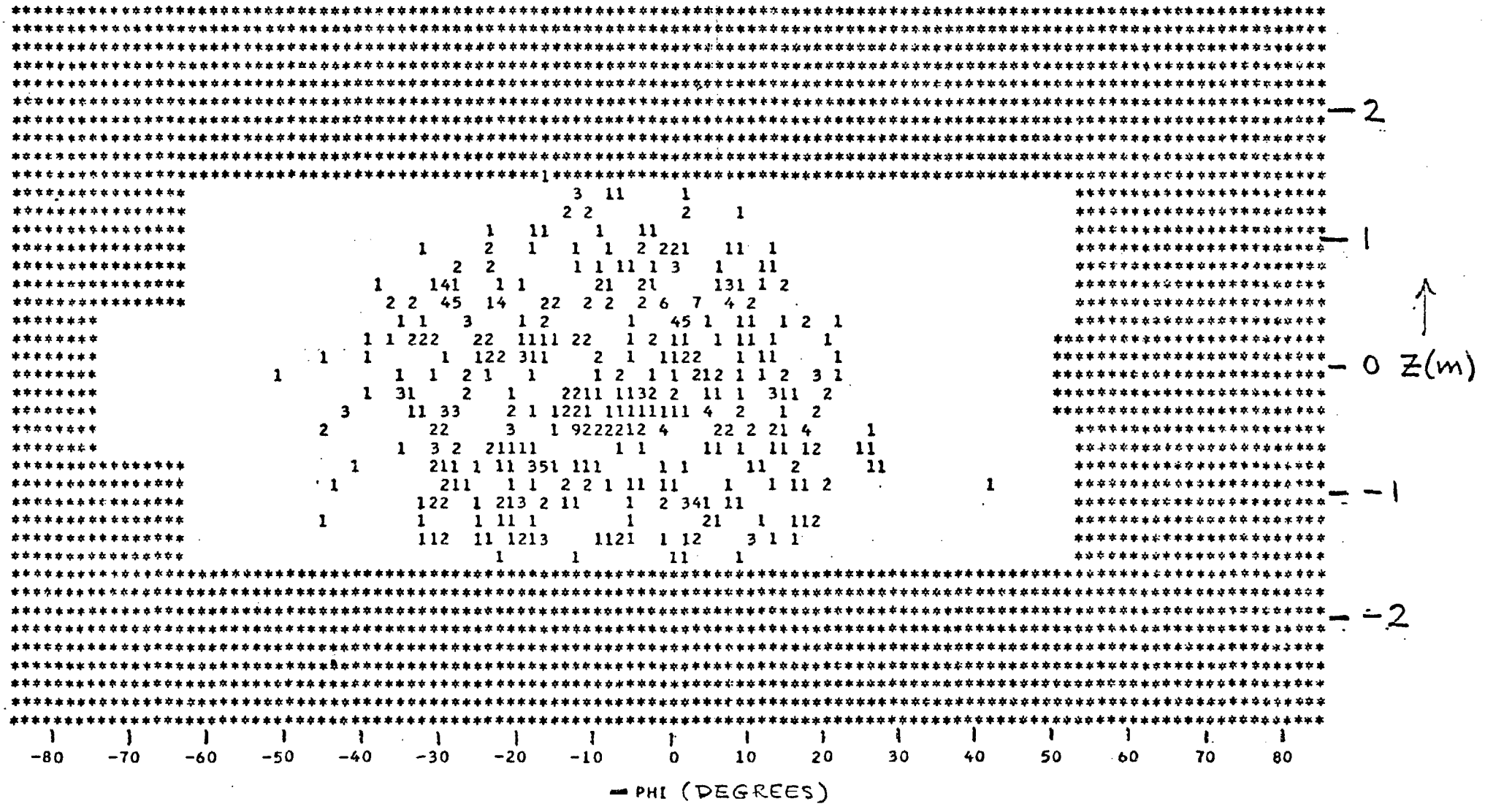

AT END OF INPUT TAPE READING, ELAPSED CP TIME IS 84.463 SEC.

Fig. 5

9A-62

END OF DATA INPUT PHASE. KIOWA HAS PROCESSED A TOTAL OF 492 EVENTS FROM GETUM.1

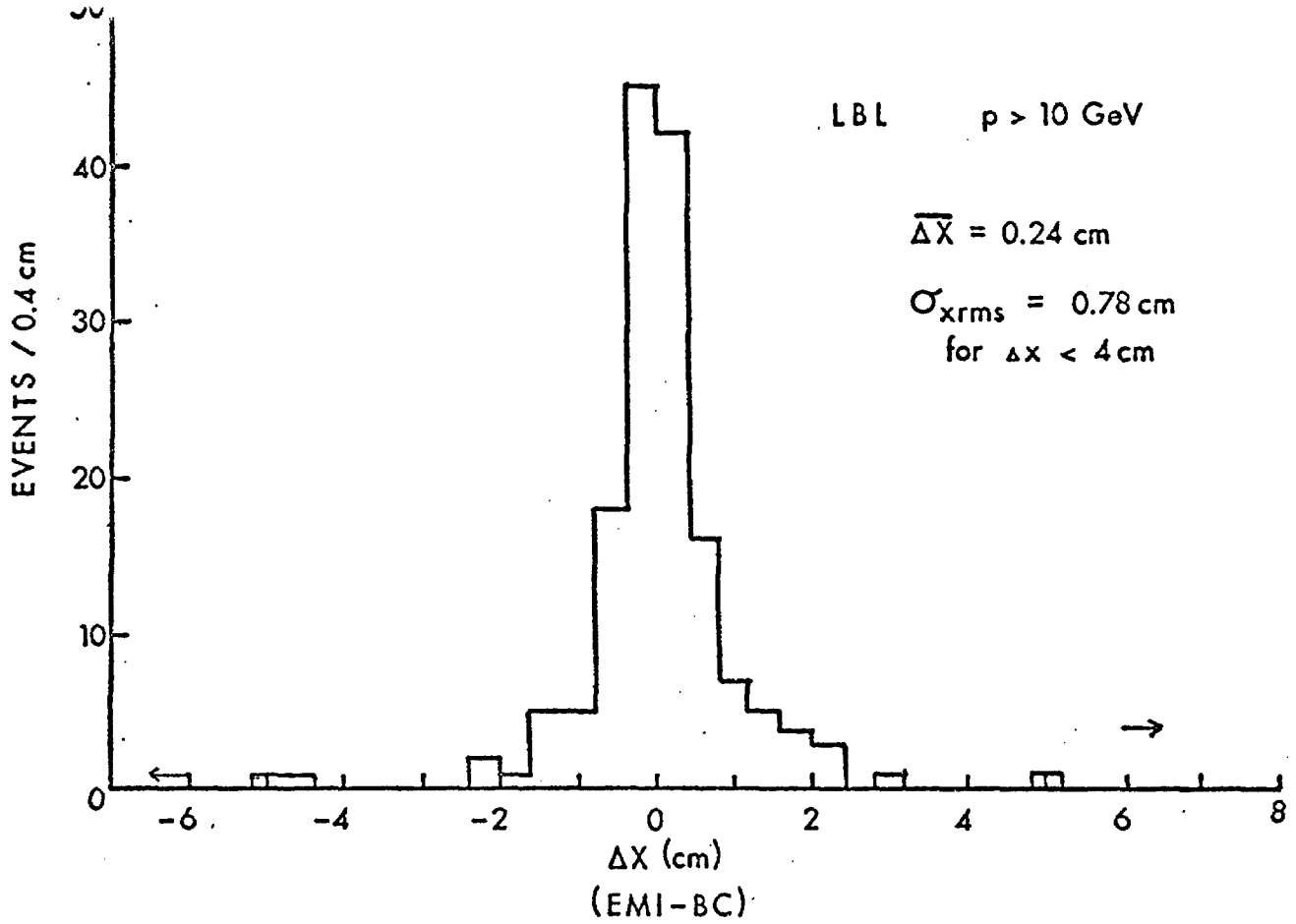
LBL
p > 10 GeV
$\overline{\Delta X}$ = 0.24 cm
σ_{xrms} = 0.78 cm
for Δx < 4 cm
EVENTS / 0.4 cm
ΔX (cm)
(EMI-BC)

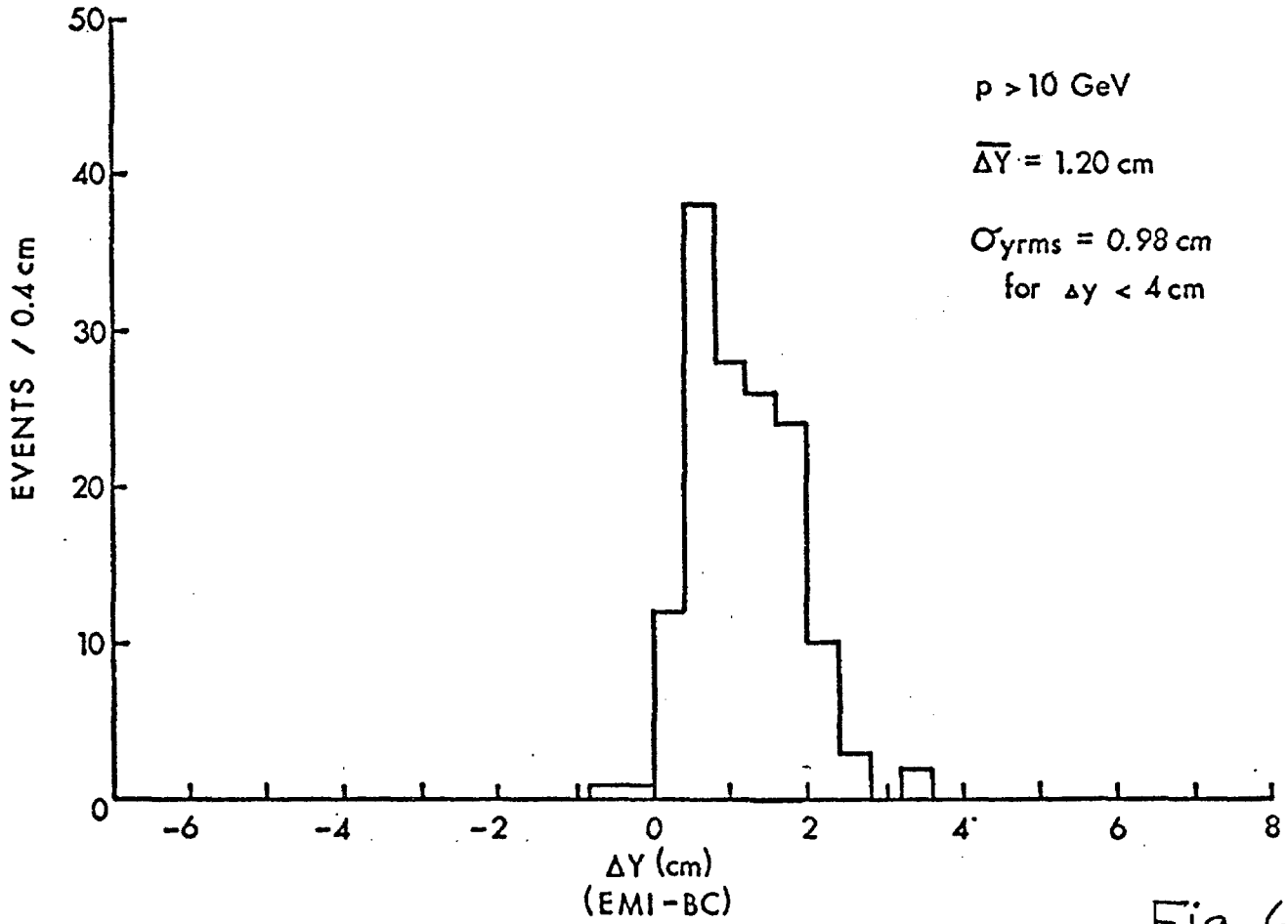
p > 10 GeV
$\overline{\Delta Y}$ = 1.20 cm
σ_{yrms} = 0.98 cm
for Δy < 4 cm
EVENTS / 0.4 cm
ΔY (cm)
(EMI-BC)

Fig. 6

NAL PROPOSAL NO. 9B Rev.

Correspondent: M.L. Stevenson

University of California
Lawrence Berkeley Laboratory
Berkeley, California 94720
Telephone: FTS 18-415-843-2740 Ext. 6301

PROPOSAL TO STUDY ANTI NEUTRINO INTERACTIONS IN THE 30 m^3 NAL BUBBLE CHAMBER WITH THE PHASE I EXTERNAL MUON IDENTIFIER

R.J. Cence, F.A. Harris, S.I. Parker, M.W. Peters
V.Z. Peterson, V.J. Stenger
University of Hawaii

A. Barbarro-Galtieri, G.R. Lynch, J.P. Marriner,
F.T. Solmitz, M.L. Stevenson
University of California
Lawrence Berkeley Laboratory

October 3, 1974

SUMMARY

We will have analyzed approximately 2500 neutrino interactions by the time the 50,000 pictures test of the Phase I External Muon Identifier (EMI) is completed (E-155). We are now requesting 300,000 pictures of the 15 foot-hybrid*-bubble chamber, filled with hydrogen and exposed to a wide band anti neutrino beam, in order to obtain a comparable number of anti neutrino interactions. We request that at least 50,000 of these anti neutrino pictures be taken during the April-May 1975 run sequence. By that time we will have analyzed 200 neutrino interactions from the copied portion of Experiment 45A film and, hopefully, 500 additional events from the 10,000 picture portion of the above mentioned test sample that we are requesting from the October-November 1974 run sequence. In this way we will make an early comparison of the hadronic final states for neutrinos and anti neutrinos on hydrogen using the wide band beam. This was the original spirit of the deferred portion of our physics proposal 9B (9 July 71) which called for 50,000 wide band events.

Most of the physics arguments and how the kinematics of anti neutrino interactions place constraints on the detectors are contained in that proposal. The first three figures of that proposal are reproduced here. The first summarizes the kinematics, the second shows pictorial momentum vector diagrams to give some idea of what a 20 GeV neutrino interaction might look like. The Landau thermodynamic model[3] was used as a "worst-case" estimate of hadron multiplicity. The third figure summarizes how the muons are bent by the magnetic field and shows why we wanted to place the EMI proportional chambers at 90° azimuth to the neutrino direction.

* With External Muon Identifier. (See reference 2)

Physics Justification

The main purpose of the experiment is to supplement the information that has been obtained by the two counter neutrino experiments,[1] namely to provide detailed information about the hadronic state of anti neutrino interactions. Muon identification is crucial to a clear understanding. The geometrical efficiency of the EMI is greater for anti neutrinos because more of their muons go forward. (See Figs 1 & 3.) Furthermore, any neutrino contamination in the anti neutrino beam can be more readily dealt with if one employs the EMI.

A. Charged lepton current

1. Although, the neutrino energy is low ($\lesssim$50 GeV) we will search for jet-like structure of the "dressed up" recoiling parton and observe how the charge-momentum distribution compares with the corresponding neutrino induced state. It is very important in this analysis to know the direction of the momentum transfer vector. Unless the muon is identified and neutral current events removed from the sample, errors will be introduced into the analysis. (See Fig. 2)

2. The known $(1-y)^2$ dependence of the anti neutrino charged lepton current cross section makes anti neutrinos very useful for searching for the production of rare, massive hadronic states. From Fig. 1, which shows lines of constant hadron invariant mass W, one observes that thresholds for massive hadronic states occur at large y and small x ($\equiv Q^2/2M\nu$) where a paucity of events occurs. Fig. 4 shows, approximately, how the 2500 events will distribute themselves in the x, y space. Here, for simplicity, we have used $\nu W_2 \propto 1-x$. Charmed particles, if they exist, are expected to have leptonic decay modes. Here, again the EMI is useful for detecting its muonic decay mode.

3. Observation of the relative rates of $\Delta S = \Delta Q$ and $\Delta S = 0$ reactions à la Cabibbo, where the final state baryon systems may not be in the same SU(3) multiplet as the proton. For example,

$$\bar{\nu} + p \rightarrow \mu^+ + \left[\Sigma^{0*}(1385) \rightarrow \begin{matrix} \Lambda \pi \\ \Sigma \pi \end{matrix} \right] , \quad \Delta S = \Delta Q$$

$$\bar{\nu} + p \rightarrow \mu^+ + \left[\Delta^0(1235) \rightarrow N \pi \right] , \quad \Delta S = 0$$

Here, there is a greater chance for misidentifying the muon than when the baryons are in the same multiplet as the proton. The EMI will eliminate the ambiguity.

4. Test of Adler's relation,

$$\lim_{E_\nu \rightarrow \infty} \frac{d\sigma(\bar{\nu}p)}{dQ^2} - \frac{d\sigma(\nu p)}{dQ^2} = \frac{G^2}{\pi} \left(\cos^2\theta_c + 2\sin^2\theta_c \right)$$

B. <u>Neutral lepton current.</u>

1. Although the neutral lepton current events can be identified in approximately 20 or 30% of the cases we have little chance of being able to determine x and y for them because of our inability to measure the energy-momentum of the neutral portion of the hadronic state. We will, however, try to extract the maximum amount of information from the charged portion. We are submitting a separate proposal to use the EMI with a light mixture of Ne in the hydrogen bubble chamber so as to be able to measure x and y.

2. Neutron background studies are crucial to an ultimate understanding of neutral current physics. We intend to search for anti neutrino interactions in the surrounding super conducting coils where the associated neutron interacts in the bubble chamber. From this we will be able to estimate the neutron background.

C. Possible Surprising Physics

With a detector system that maximizes particle identification, one is best able to detect unusual processes.

Apparatus Needed

A. 15' -- Hydrogen filled bubble chamber.

B. External Muon Identifier.

The twenty-five $1m^2$ - multiwire proportional chambers (MWPC) envelope the downstream portion of the 22' diameter vacuum tank. Fig. 5 summarizes the geometrical coverage of the 22 MWPC's used during the July-Aug 74 run of E45A. It shows the vertical and azimuthal coverage as viewed by an observer at the center of the bubble chamber. The plotted points are the predicted hit positions in the MWPC of incoming regenerated muons (from the berm and earth shield) that traverse the visible volume of the bubble chamber. Fig. 6 shows the deviation of the measured position in the EMI from the predicted one.[2] The RMS deviation is very nearly that expected from multiple scattering in the four interaction lengths absorber between the bubble chamber body and the MWPC's. More than 80 percent† of the observed hits fall within the "96% circle" centered at the predicted point. Less than two percent of these incoming tracks interact; consequently, they are mostly muons. Details of this earlier run (400 GeV triplet load) are given in TM513.[2]

C. Neutrino Beam Monitoring Equipment.

D. We would like to assist Experiment 31A (Derrick) in determining the effectiveness of the plug that is likely to be first installed for the April-May 75 run. We plan to operate the EMI during a reasonable fraction of E-31A's exposure in Oct-Nov 74.

E. Scan Projector suitable for monitoring the quality of the bubble chamber pictures from the test strips.

† Some of the beam spill was known to be out of time with the EMI gate during this early run.

Scope of the Experiment

1. 50,000 of 300,000 anti neutrino pictures to be taken during the April-May 1975 run sequence.
2. The remaining 250,000 pictures to be acquired as the schedule permits.
3. At this early stage of bubble chamber operation we shall assume that 30,000 pictures can be accumulated per week. The first 50,000 pictures will take about two weeks, and the remaining 250,000 another eight weeks.
4. Very little testing of equipment is required. We assume implicitly that all beams that are capable of producing neutron or charged background in the bubble chamber will have their spill times not during the bubble chamber sensitive time.

REFERENCES

1. NAL Experiment 21, California Institute of Technology - NAL Group. NAL Experiment 1A, Harvard-Pennsylvania-Wisconsin Group.

2. "Matching 'Muon' Tracks in The 15' Bubble Chamber To The EMI Proportional Chambers", University of Hawaii-LBL Group; Experiment 155, TM-513 (10 October 1974).

"Surveying The External Muon Identifier and The 15' Bubble Chamber With 250 GeV Mesons", TM-509 (16 July 1974), University of Hawaii-LBL Group.

Complete details of the construction and electronics of the MWPC's and an early test of muon identification are found in the following references:

a) NAL Proposal 155, "Development and Test of an External Muon Identifier for the 30 m^3 Bubble Chamber", R.J.Cence, F.A.Harris, S.I.Parker, M.W.Peters, V.Z.Peterson, V.J.Stenger, D.E.Yount; (UH) A.Barbarro-Galtieri, J.P.Marriner, F.T.Solmitz, M.L.Stevenson; (LBL) V.Z.Peterson, Proceedings of 1973 International Conference on Instrumentation for High Energy Physics at Frascati, Italy; "Hybrid Bubble Chamber Detection of Neutrino Events - The External Muon Identifier".

b) "Muon Identification Using Multiwire Proportional Chamber", F.A.Harris, S.I.Parker, V.Z.Peterson, D.E.Yount, M.L.Stevenson; Nuclear Instruments and Methods 103, 345 (1972).

c) "EMI Development - Half Meter Proportional Chamber Test Results", S.I.Parker and R.Jones, NAL TM-359, LBL 797, UH-511-122-72.

d) "Digitizing Electronics for the EMI Multiwire Proportional Chambers", E.Binnall, F.Kirsten, K.Lee and C.Nunnally, NAL TM-360, LBL 798.

3) For a recent discussion of this model see J.D.Bjorken and B.L.Ioffe "Annihilation of e^+e^- into Hadrons" SLAC-PUB-1467 (T/E) August 1974. (To be published in Izv. Acad. Nauk, SSSR, Ser. Fiz.)

FIGURE CAPTIONS

Figure 1. The kinematics of inelastic lepton scattering are summarized here. The solid lines radiating from $Q^2=0$, $\nu(=\nu_{max}=E)$ are loci of equal final lepton scattering angle. The parallel solid lines are loci of equal invariant final state hadron mass. They also show "worst case" predictions of hadron multiplicity. The radial line originating at $Q^2=0$, $\nu=0$ are loci of constant $x(=Q^2/2M\nu)$. The dashed curves are loci of constant Lorentz factors, γ_W of the hadron system.

Figure 2. Typical momentum vector diagrams for various regions in the x, y space are shown. The opening angles of the cones are typical of those expected of the Landau Thermodynamical model. A jet-like model would predict opening angles and multiplicities much smaller than these.

Figure 3. Typical Muon Trajectories in the 30 kG field of the 15' chamber are shown. The two solid curves for each (x,y) are the extremes for muons produced in the equatorial plane. The dashed curve is that for a muon emitted with its extreme dip value.

Figure 4. This figure shows approximately how the 2500 anti neutrino events will populate the x,y space.

Figure 5. The azimuthal and vertical coverage of the EMI, as viewed by an observer at the center of the bubble

chamber, is summarized here. It also shows where regenerated muons (from the rear portion of the 1000 meter earth shield) are predicted by the bubble chamber measurements to strike the EMI.

Figure 6. Summary of the deviation of the measured position of muons in the EMI from the predicted position using the bubble chamber picture. x is horizontal and y is vertical.

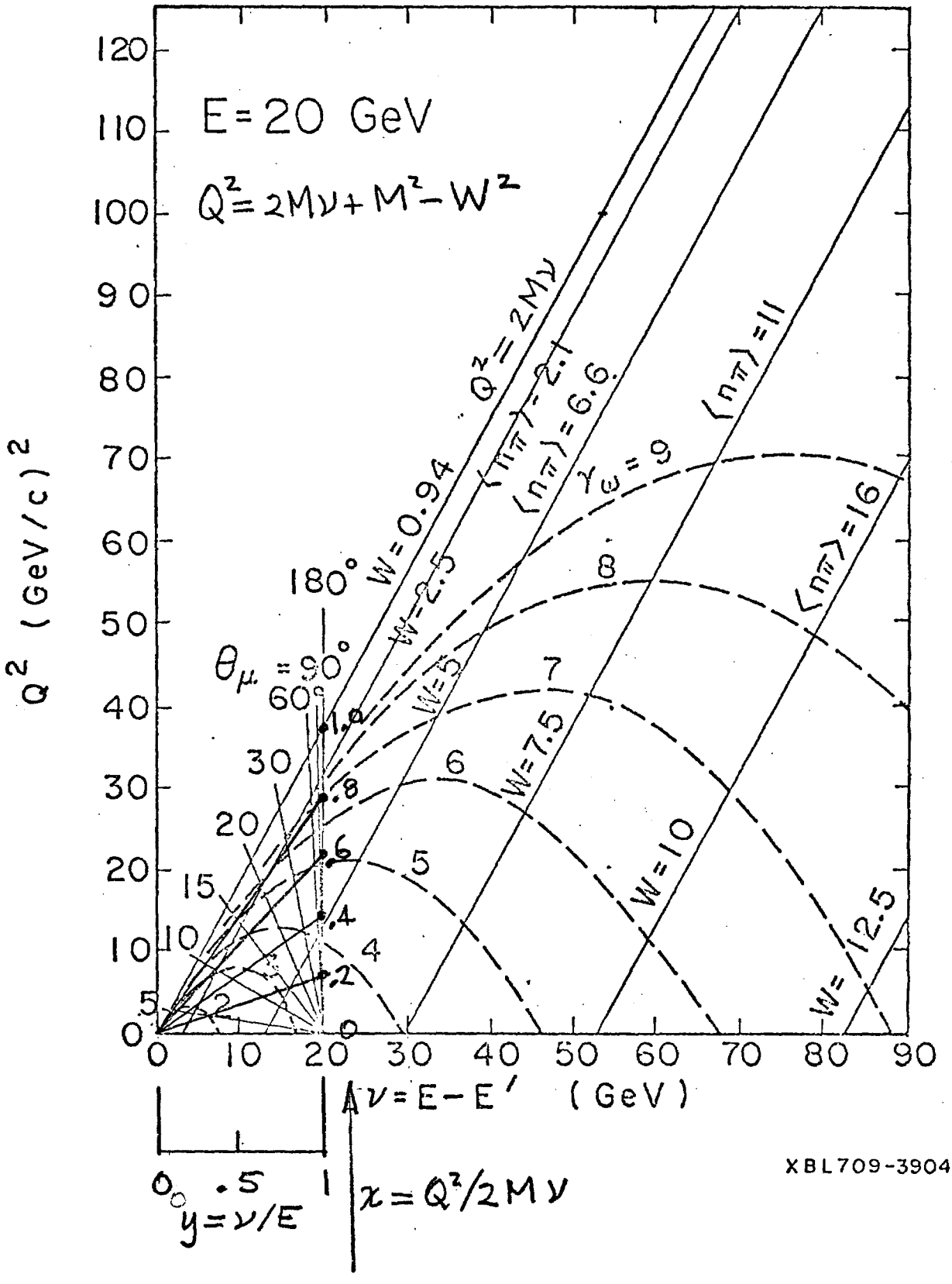
E = 20 GeV
$Q^2 = 2M\nu + M^2 - W^2$
$Q^2 = 2M\nu$
W = 0.94
W = 2.5
W = 5
W = 7.5
W = 10
W = 12.5
$\langle n\pi \rangle = 2.1$
$\langle n\pi \rangle = 6.6$
$\langle n\pi \rangle = 11$
$\langle n\pi \rangle = 16$
$\gamma_\omega = 9$
$\theta_\mu = 90°$
180°
60°
30
20
15
10
5
2
1.0
.8
.6
.4
.2
0
4
5
6
7
8
Q^2 (GeV/c)^2
$\nu = E - E'$ (GeV)
$y = \nu/E$
$x = Q^2/2M\nu$
XBL709-3904

FIG. 1

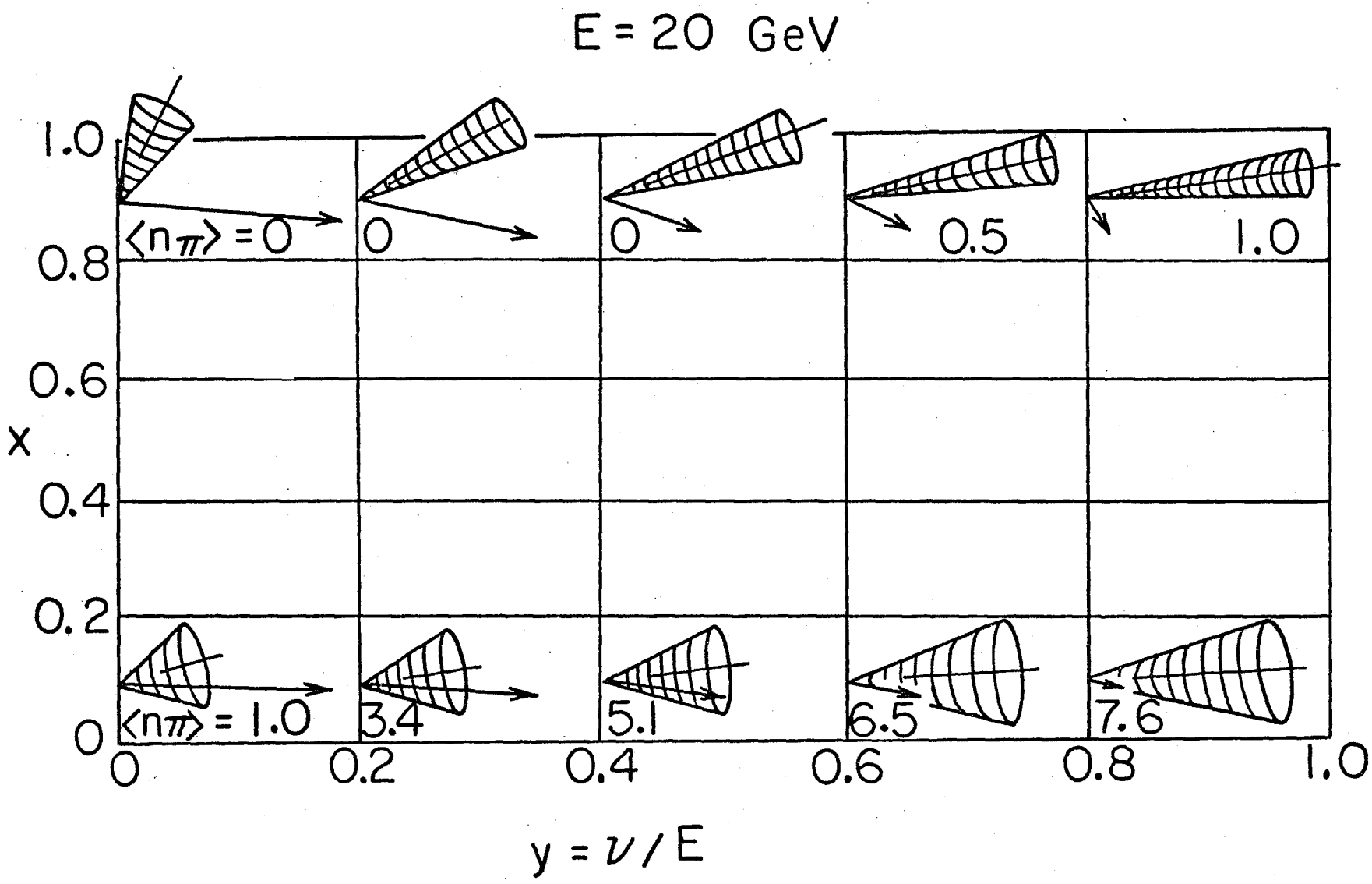

XBL709-3896

FIG. 2

Muon Trajectories

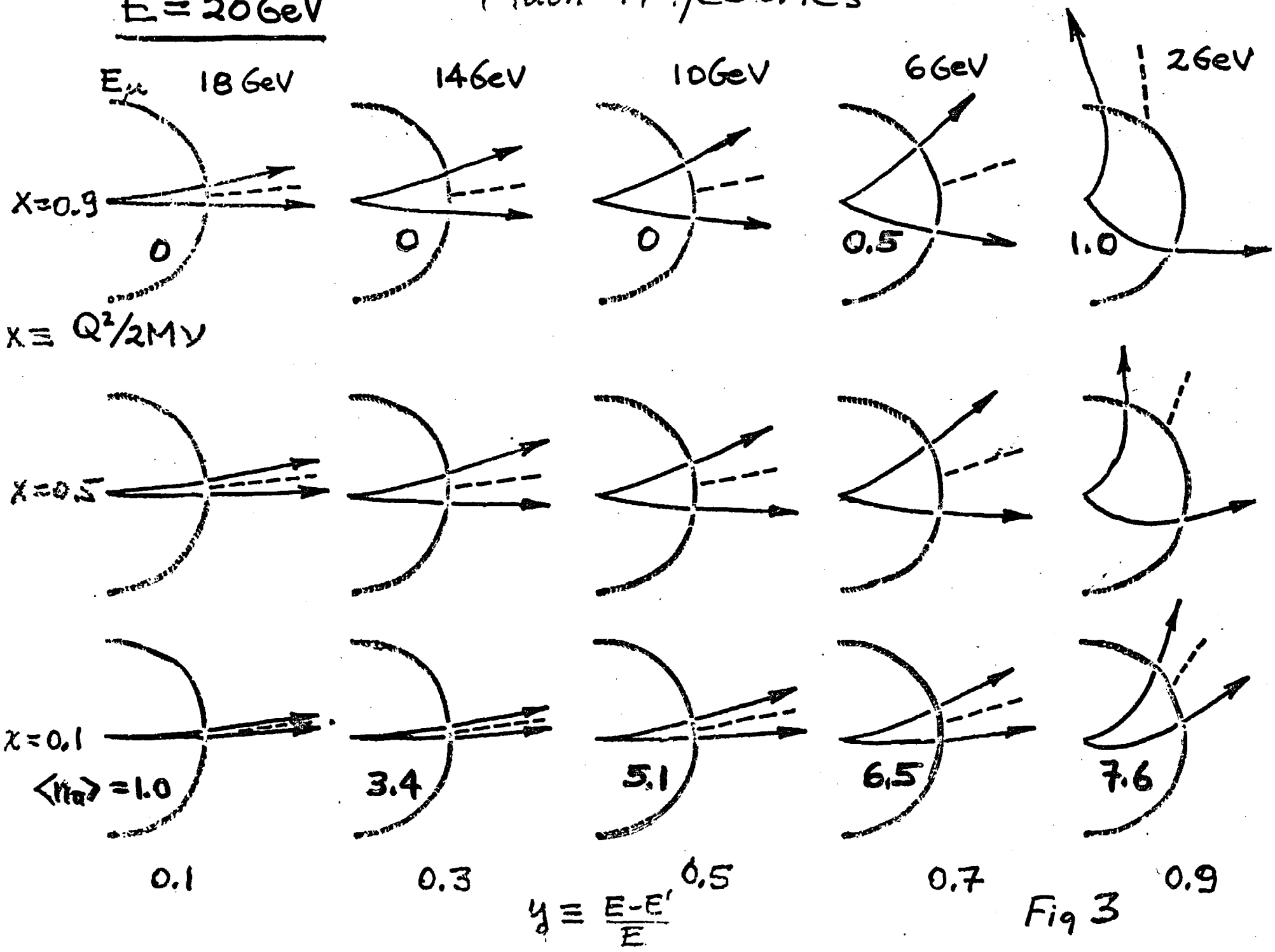

Fig 3

Distribution of 2500 events

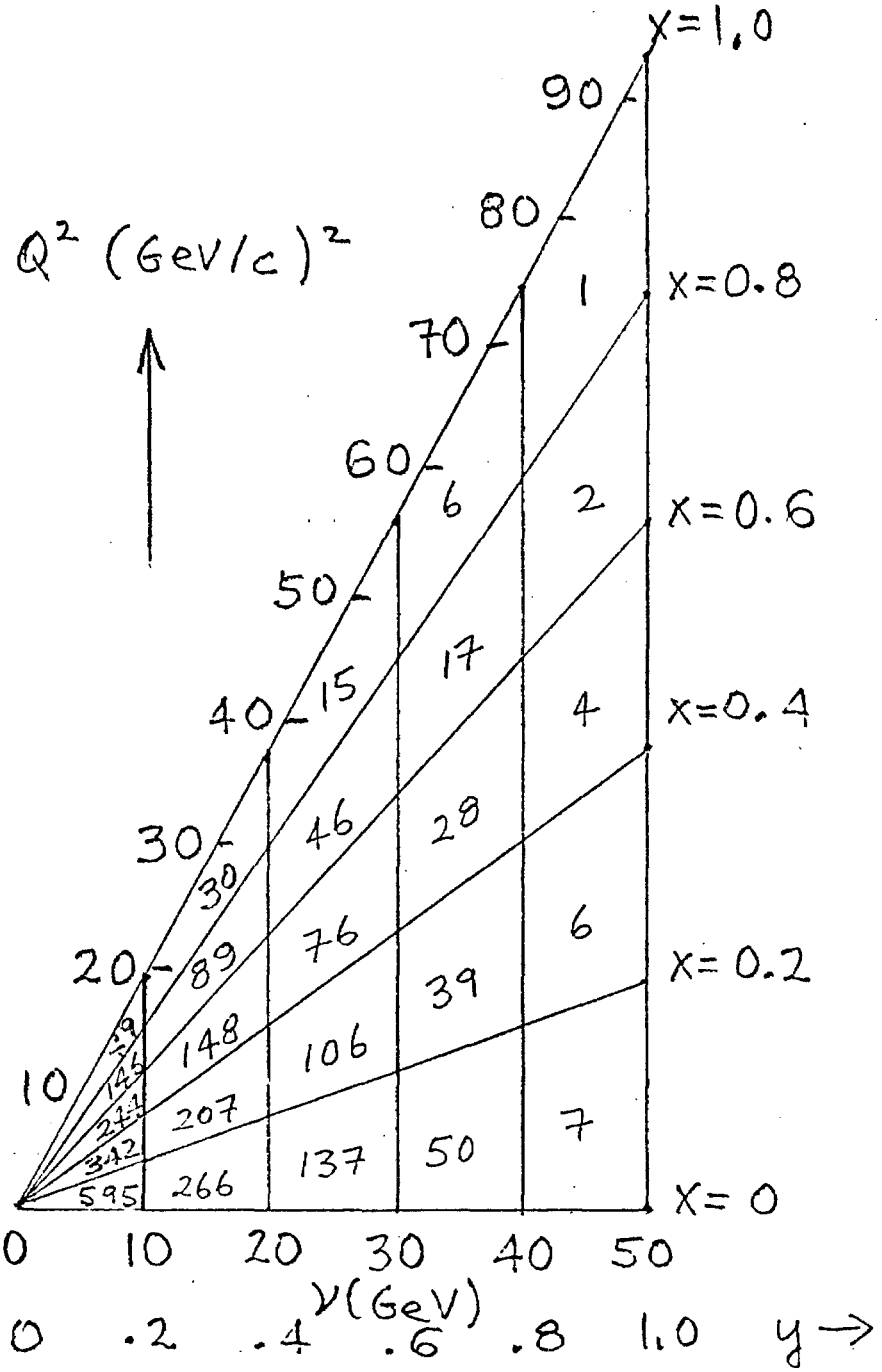

$$\frac{d^2\sigma}{dx\,dy} \approx \frac{G^2 ME}{\pi}\,\frac{Q^2}{2\pi}(1-x)\left\{\sigma_L + (1-y)\sigma_S + (1-y)^2\sigma_R\right\}$$

with $\underline{\sigma_L = \sigma_S = 0}$. $\sigma_{L,S,R}$ ARE HELICITY CROSS SECTIONS

Fig 4

CHAMBER NUMBERS

0	25	20	9	17	21	19	18	0
16	14	4	22	2	15	3	23	0
0	11	8	5	10	7	13	12	0

NUMBER OF HITS

0	0	10	26	46	20	0	0	0
0	4	31	48	68	47	11	0	0
0	2	22	61	49	41	9	1	0

$|p| > 5$ GeV/c

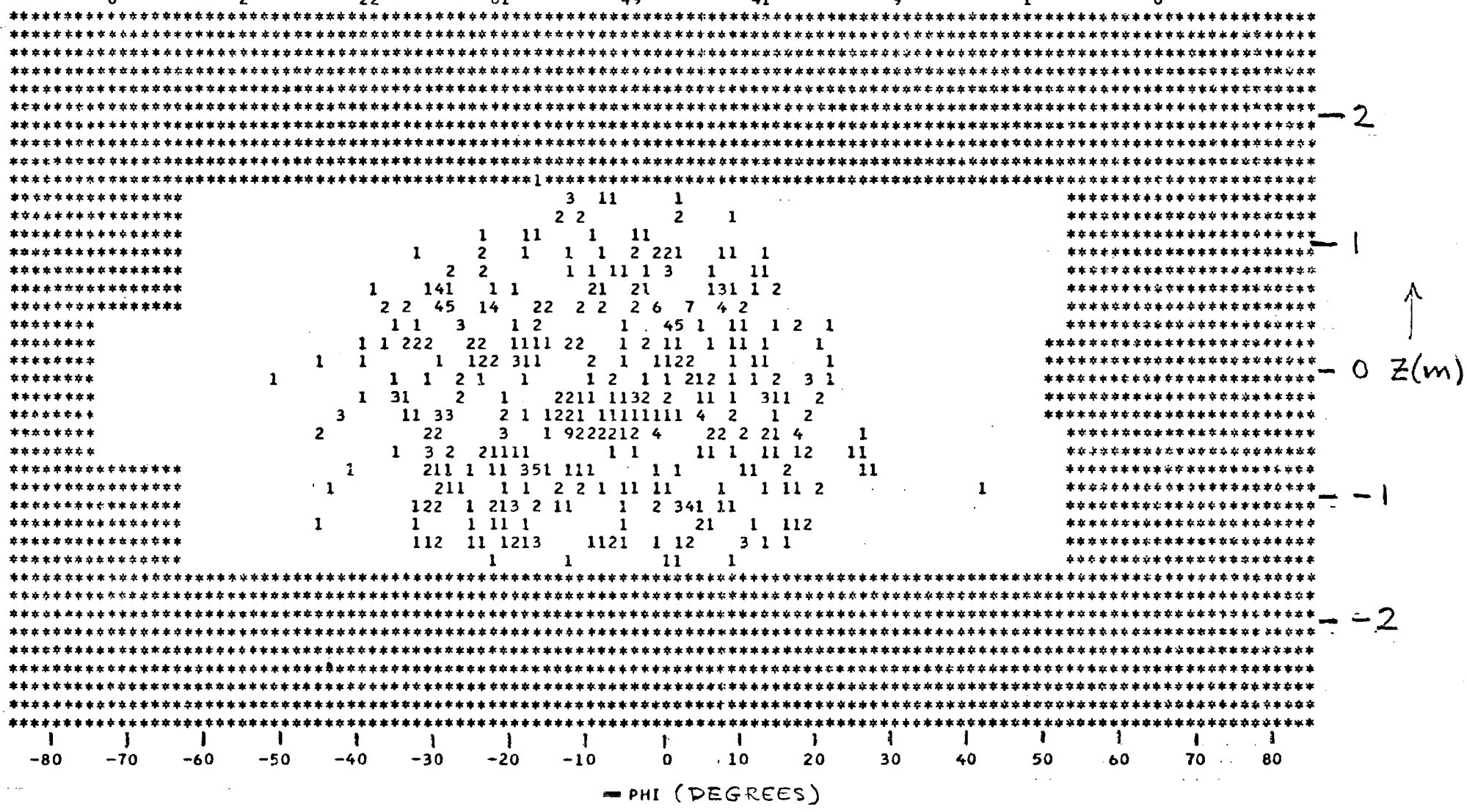

AT END OF INPUT TAPE READING, ELAPSED CP TIME IS 84.463 SEC.

Fig. 5

END OF DATA INPUT PHASE. KIOWA HAS PROCESSED A TOTAL OF 492 EVENTS FROM GETUM.1

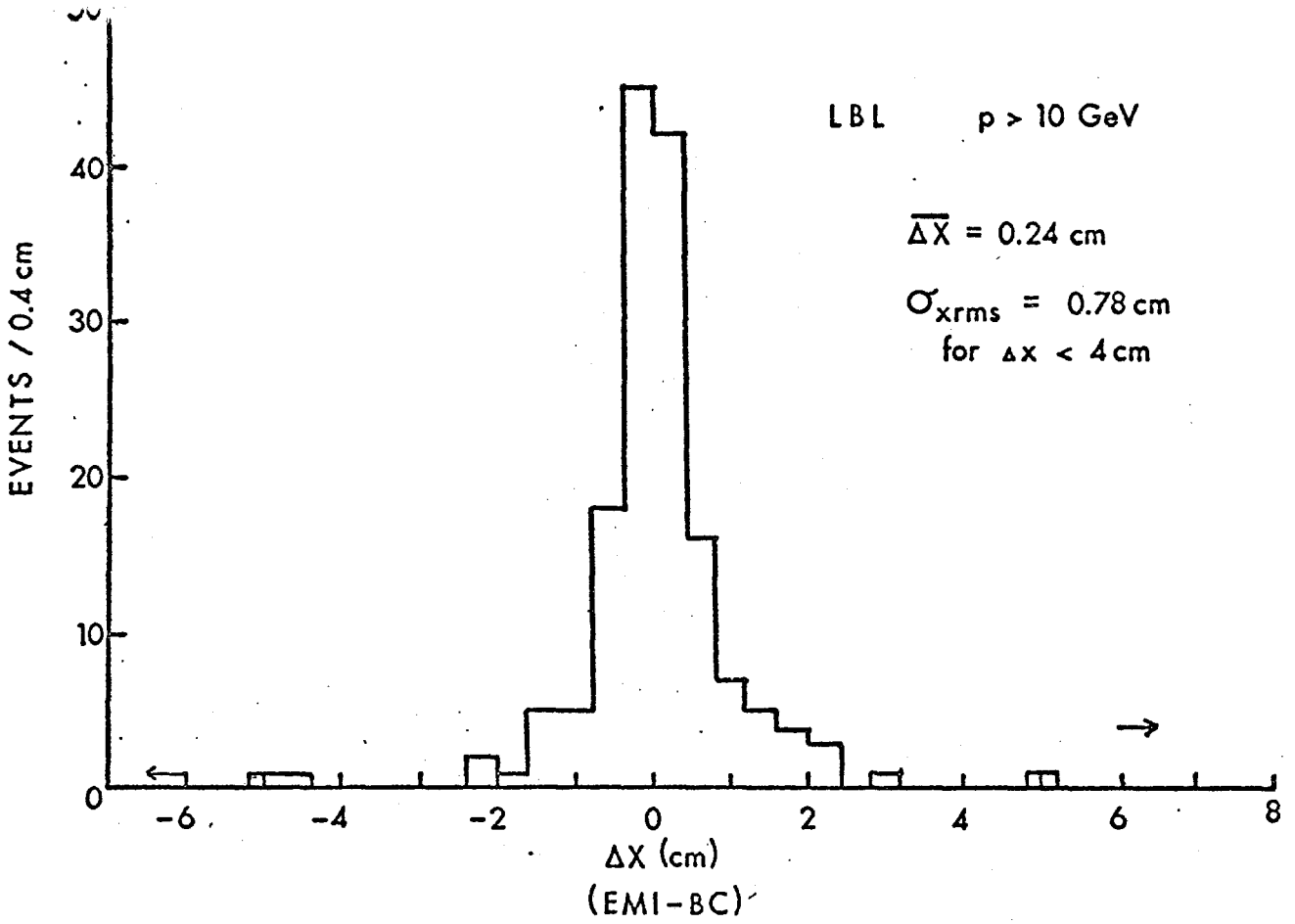

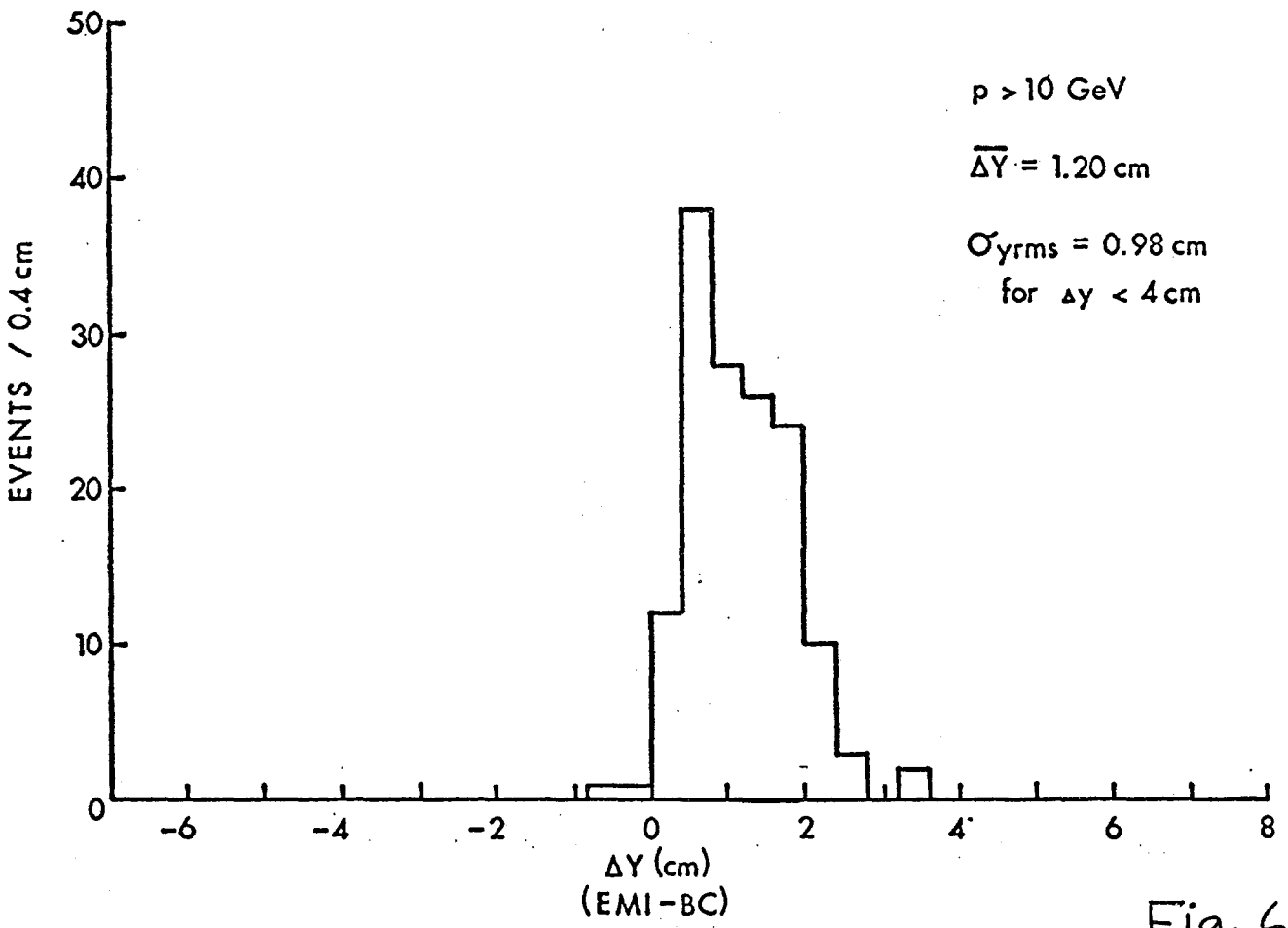

Fig. 6

~~Figure 3a~~